X-ray Reverberation
from a

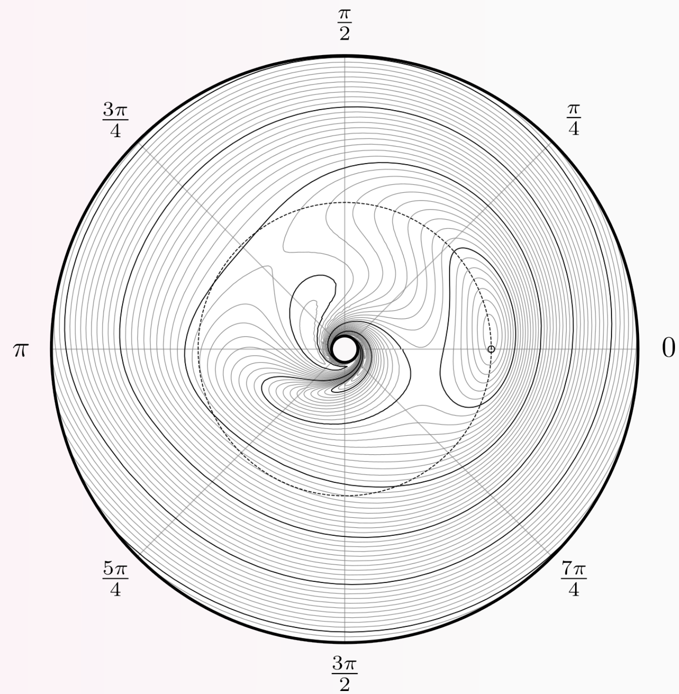

Ring-like Corona

Fergus Baker (he/him) <fergus.j.baker@durham.ac.uk>

Adam Ingram, Guglielmo Mastroserio, Benjamin Ricketts, Matteo Lucchini.

Many Tones of Accretion
07 September 2026

Durham University

European Research Council
Established by the European Commission

XMAPS

Revision: 75583e6c2c716afbfc57aaedc06d1a4b268c5637

X-ray reverberation

e.g. Fabian et al. (1989); Reynolds et al. (1999);
Zoghbi et al. (2012); Uttley et al. (2014);
Chainakun et al. (2016)

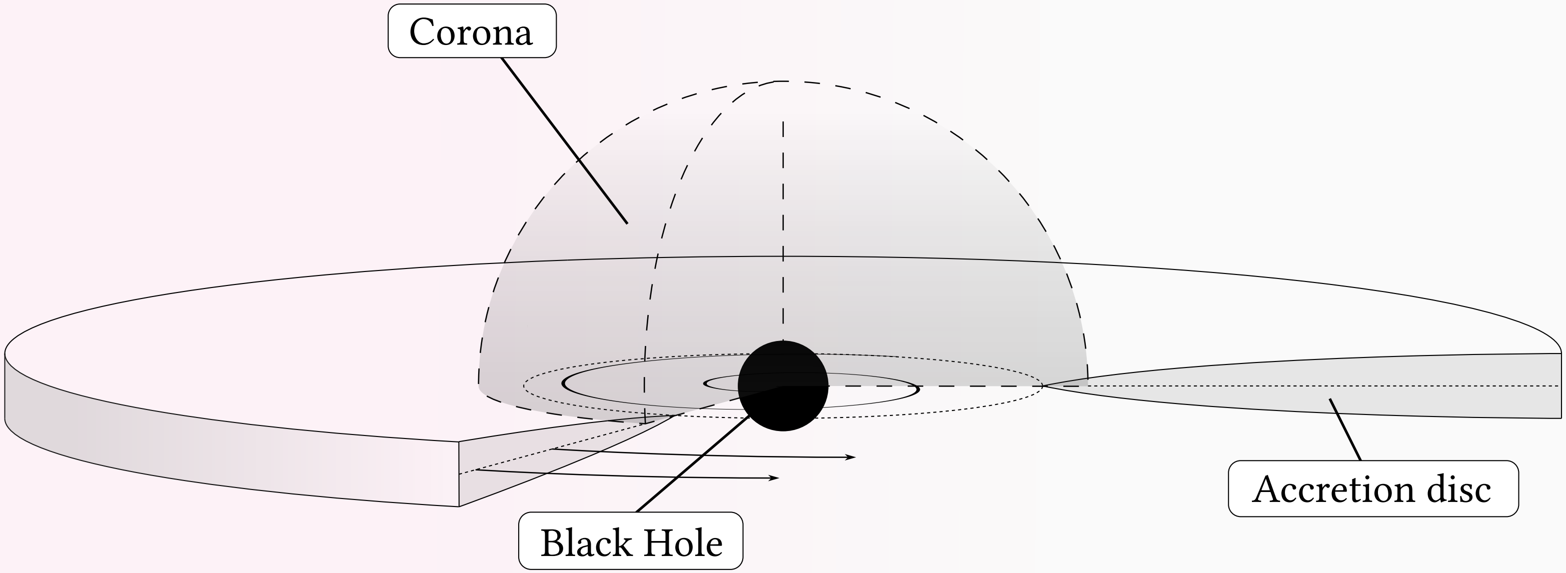

X-ray reverberation

e.g. Fabian et al. (1989); Reynolds et al. (1999); Zoghbi et al. (2012); Uttley et al. (2014); Chainakun et al. (2016)

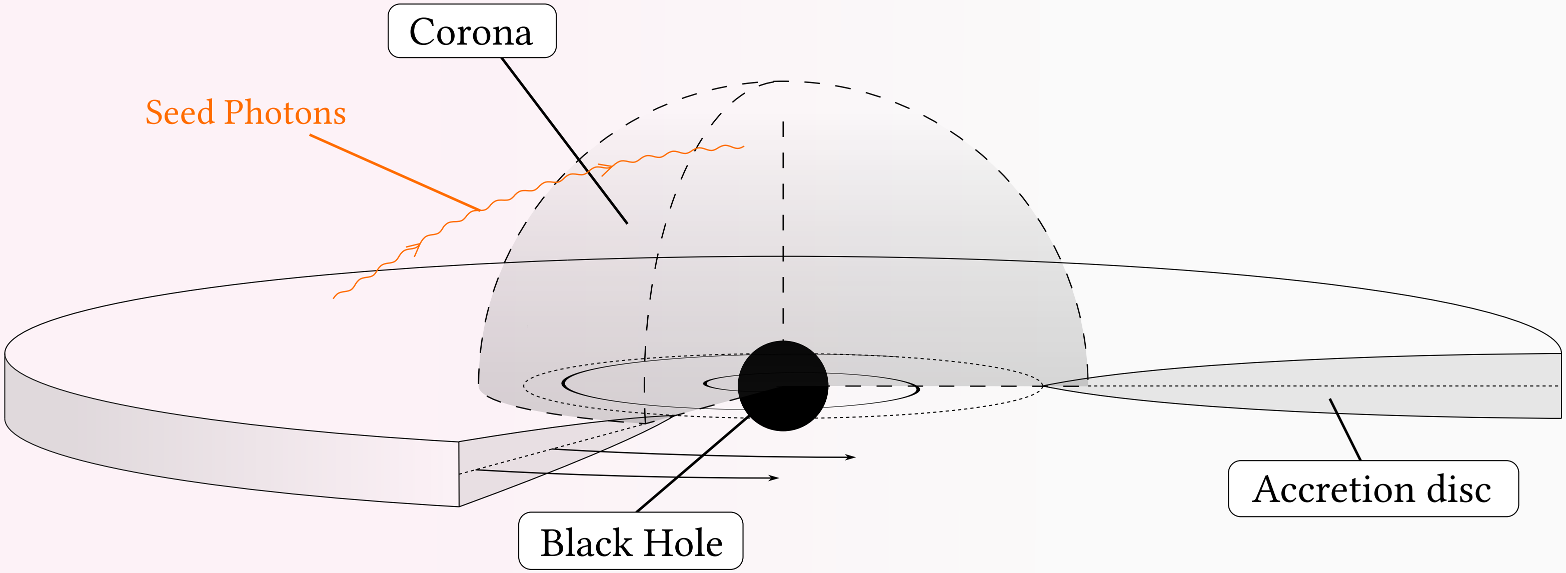

X-ray reverberation

e.g. Fabian et al. (1989); Reynolds et al. (1999); Zoghbi et al. (2012); Uttley et al. (2014); Chainakun et al. (2016)

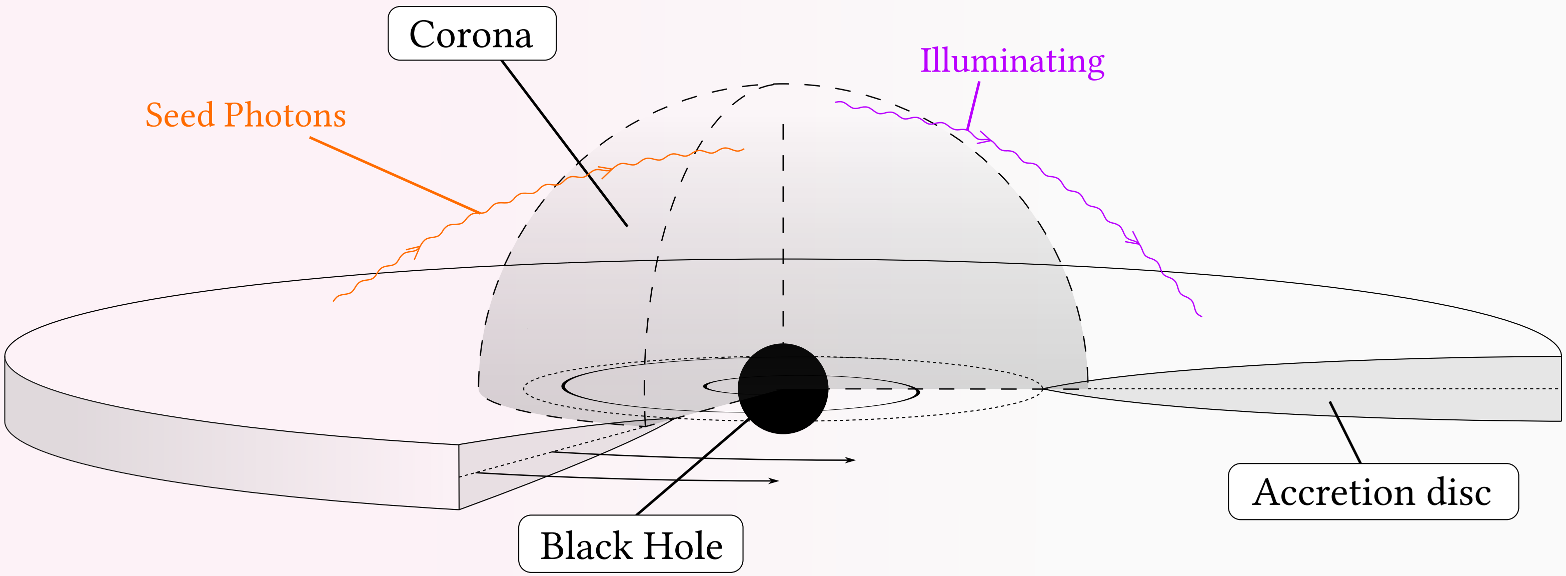

X-ray reverberation

e.g. Fabian et al. (1989); Reynolds et al. (1999);
Zoghbi et al. (2012); Uttley et al. (2014);
Chainakun et al. (2016)

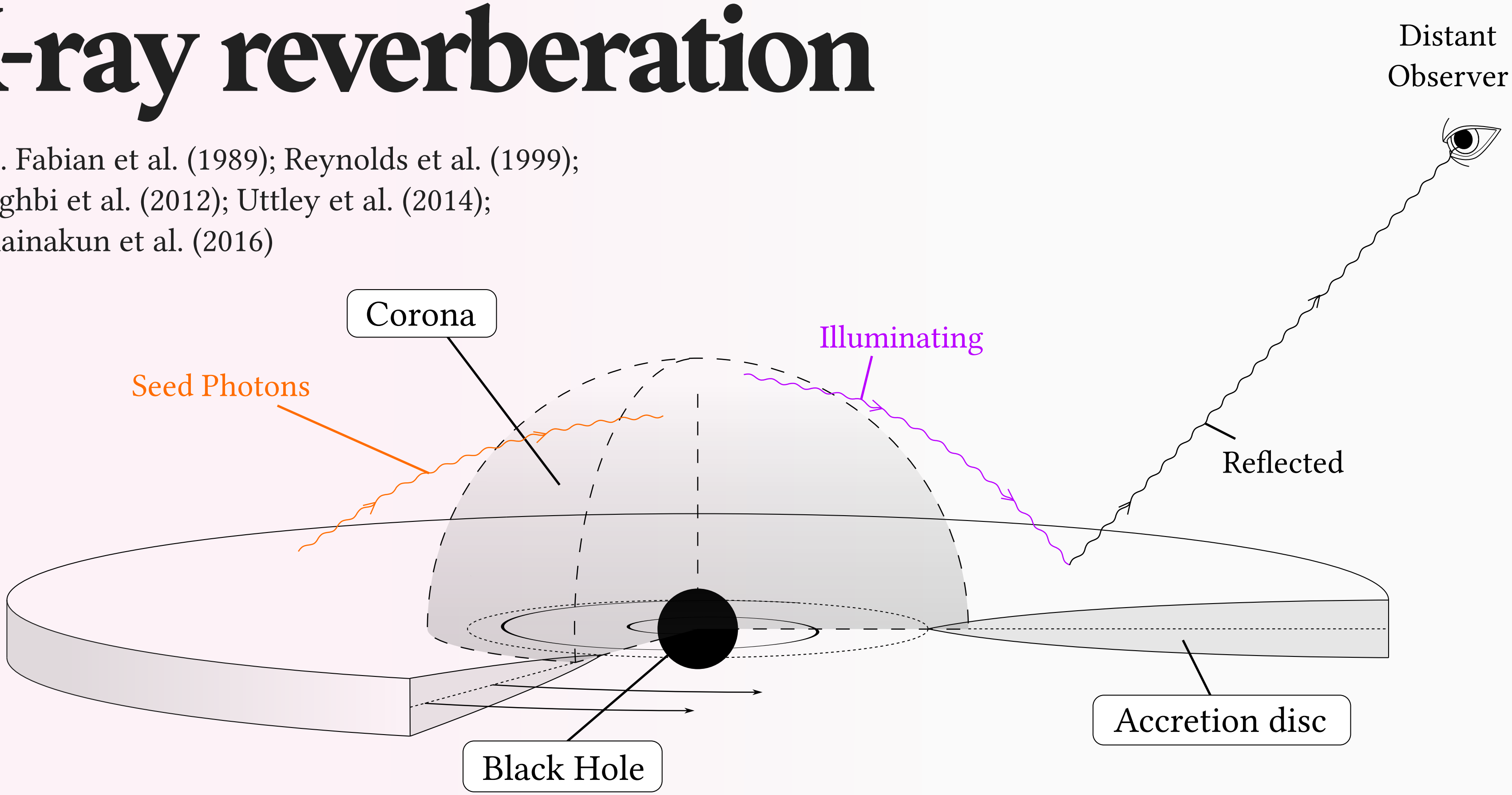

X-ray reverberation

e.g. Fabian et al. (1989); Reynolds et al. (1999); Zoghbi et al. (2012); Uttley et al. (2014); Chainakun et al. (2016)

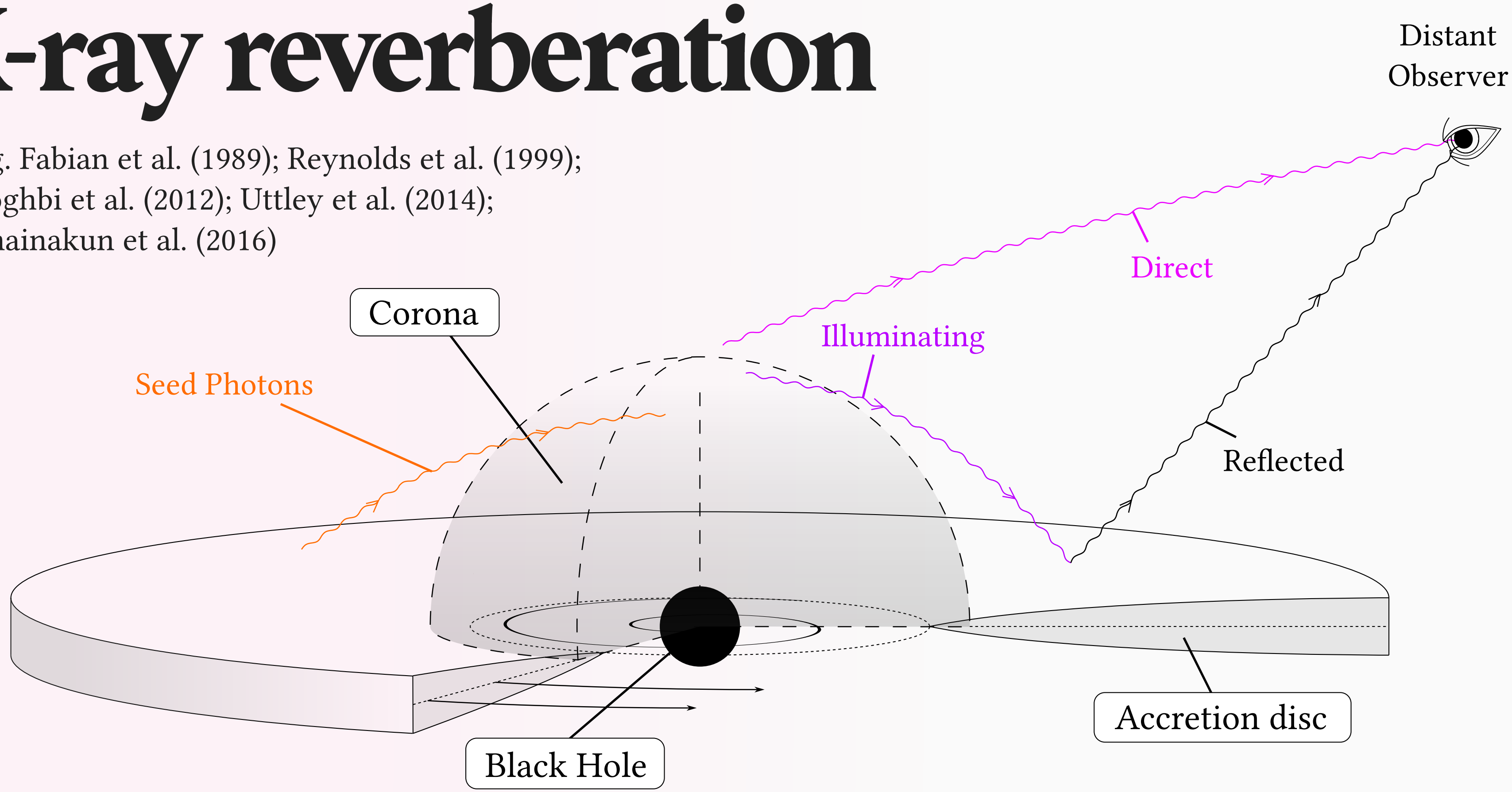

X-ray reverberation

e.g. Fabian et al. (1989); Reynolds et al. (1999);
Zoghbi et al. (2012); Uttley et al. (2014);
Chainakun et al. (2016)

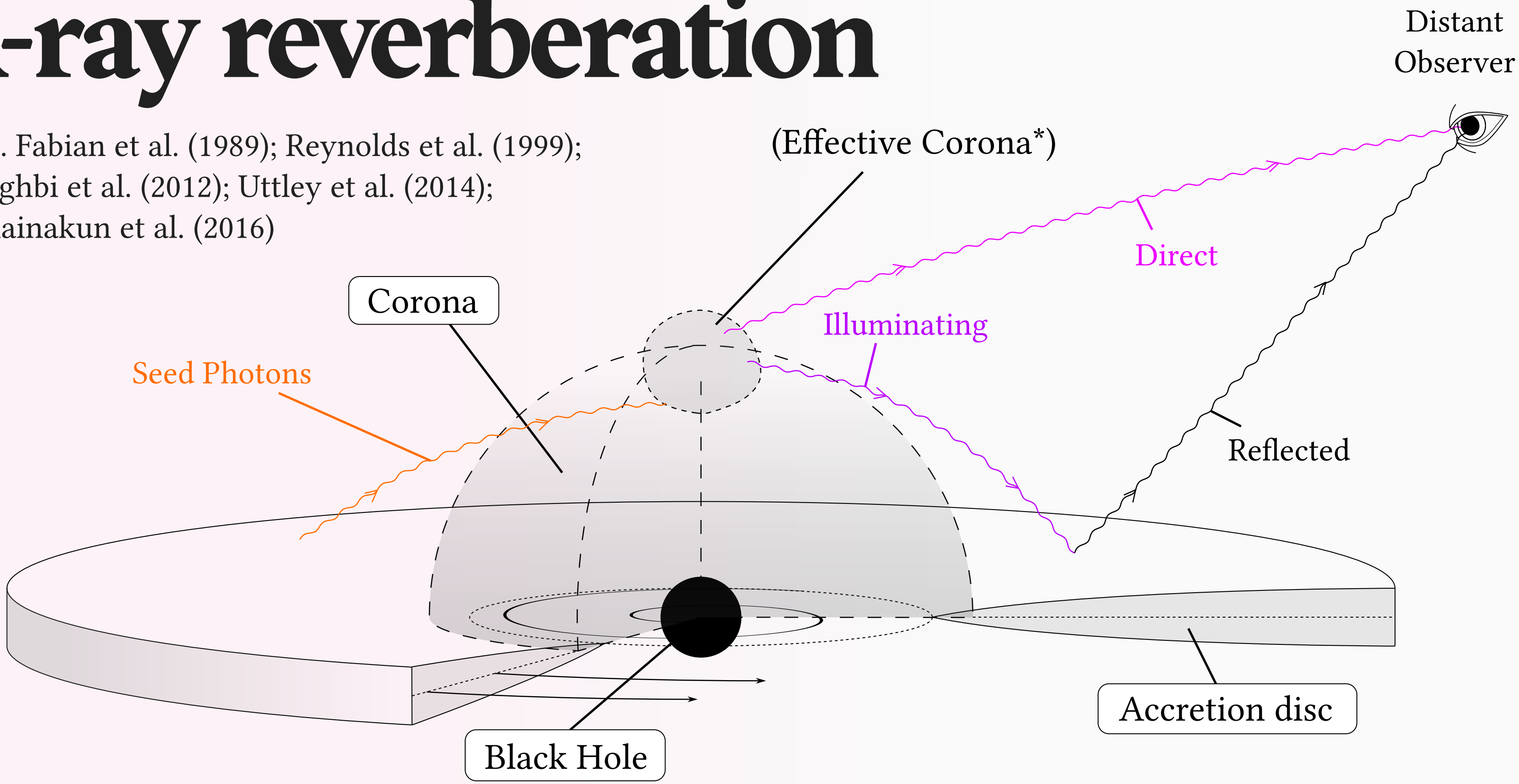

X-ray reverberation

e.g. Fabian et al. (1989); Reynolds et al. (1999);
Zoghbi et al. (2012); Uttley et al. (2014);
Chainakun et al. (2016)

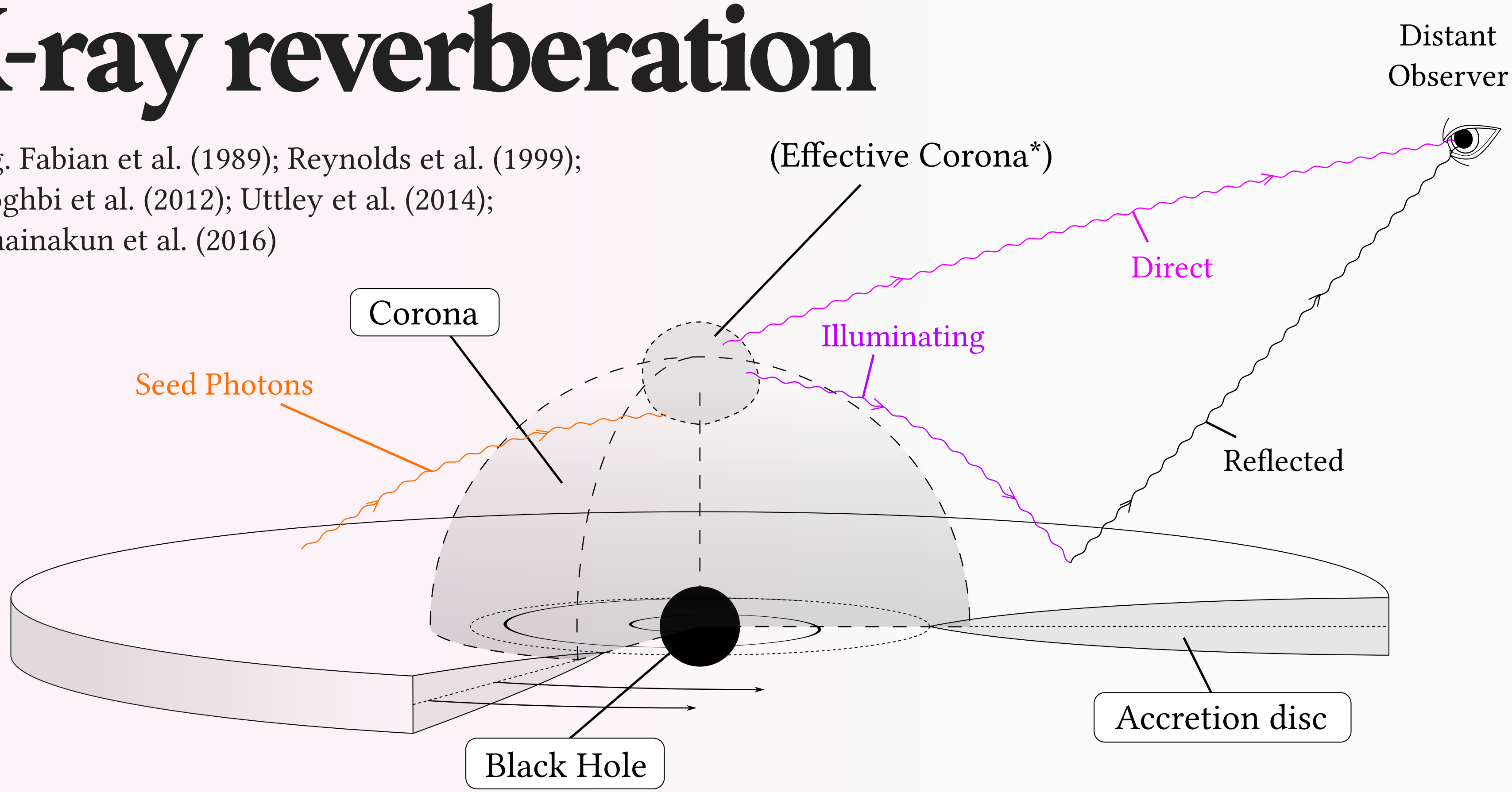

X-ray reverberation is the **time-lag** between the **direct** and **reflected** components in different **energy bands** and at different **Fourier frequencies**.

X-ray reverberation

e.g. Fabian et al. (1989); Reynolds et al. (1999); Zoghbi et al. (2012); Uttley et al. (2014); Chainakun et al. (2016)

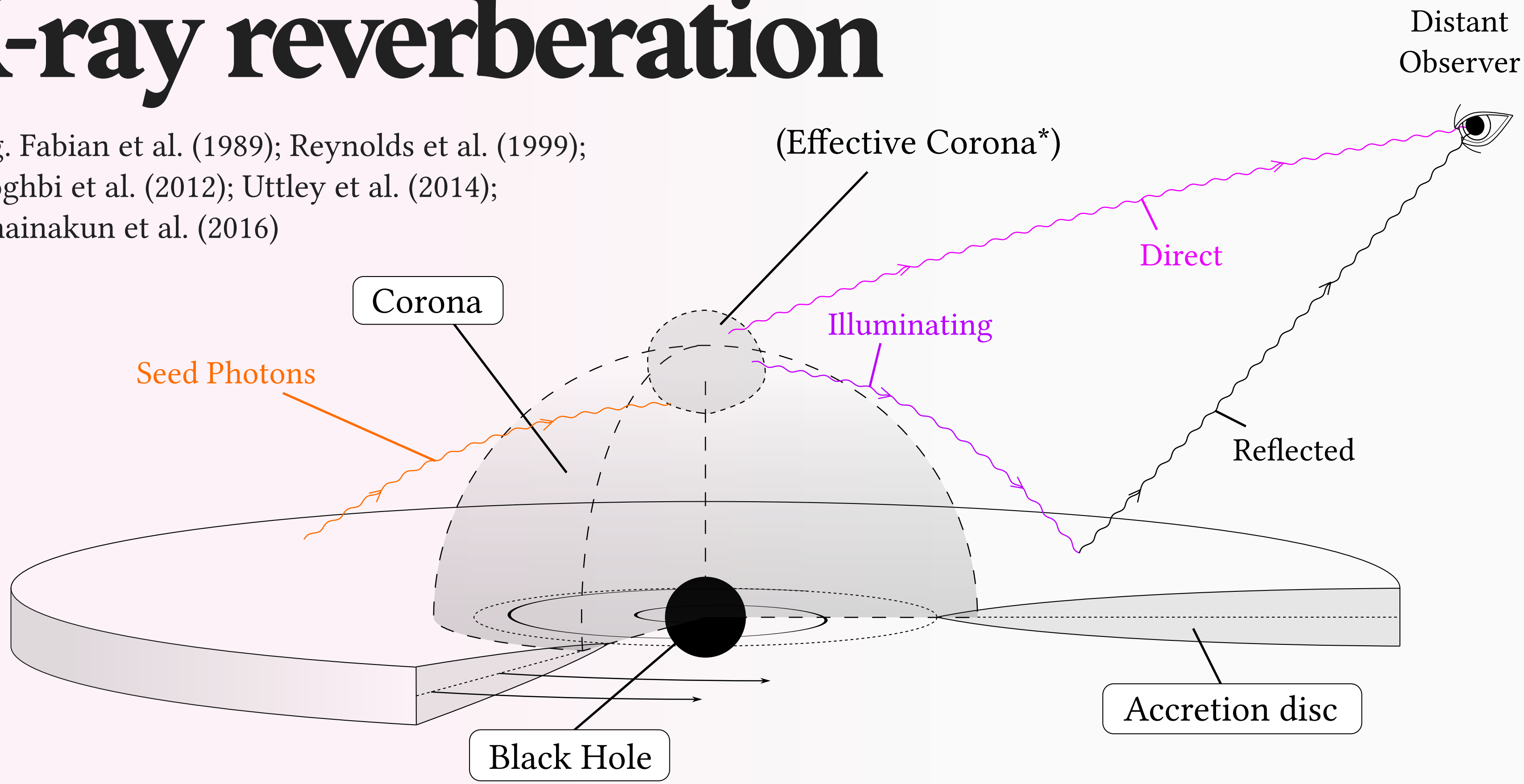

X-ray reverberation is the **time-lag** between the **direct** and **reflected** components in different **energy bands** and at different **Fourier frequencies**.

Modelled self-consistently in **Reltrans** (Ingram et al. 2019, Mastroserio et al. 2021).

- Also modelled by others, e.g. Caballero-Garcia et al. (2019)

X-ray reverberation

e.g. Fabian et al. (1989); Reynolds et al. (1999); Zoghbi et al. (2012); Uttley et al. (2014); Chainakun et al. (2016)

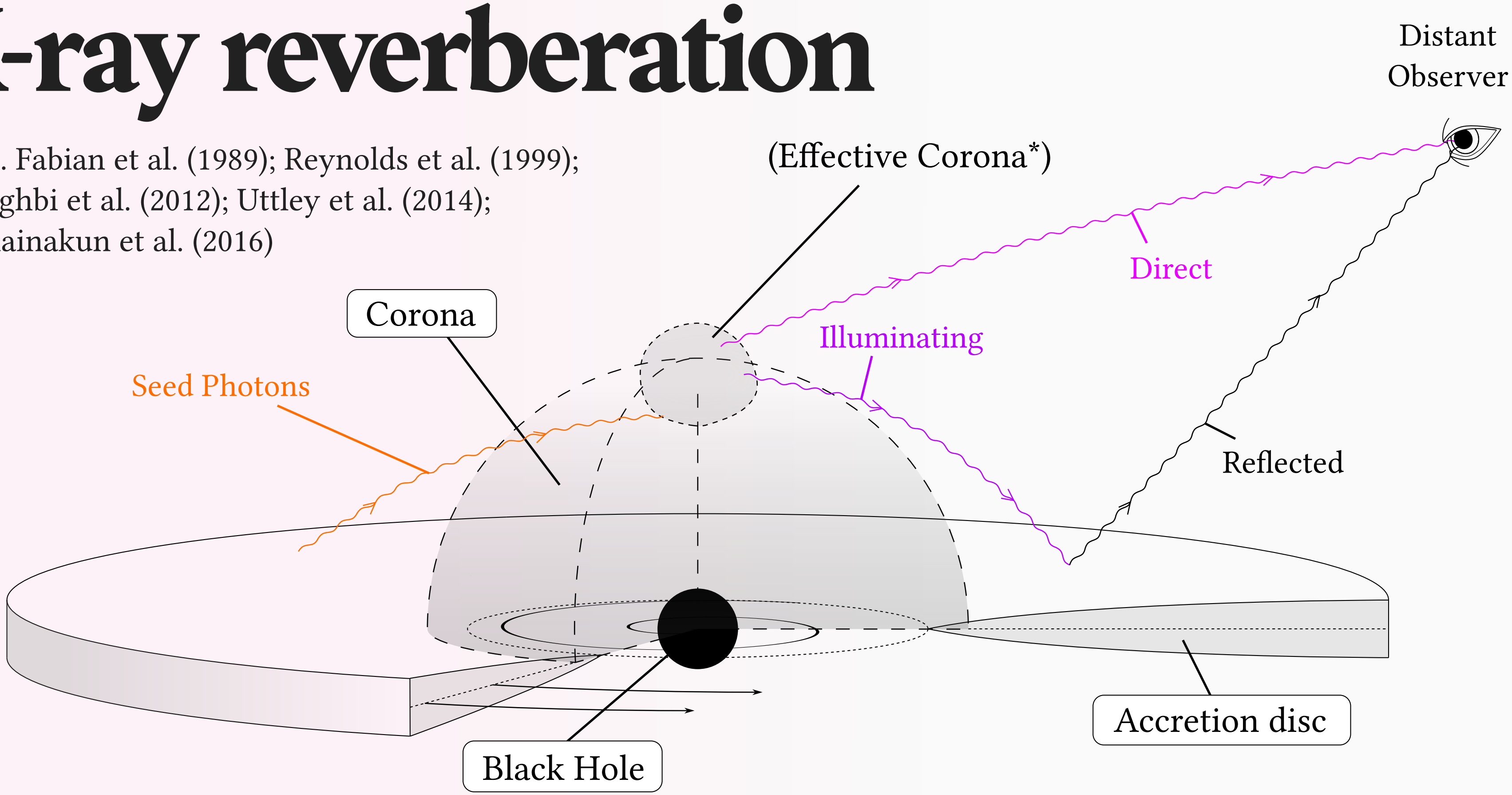

X-ray reverberation is the **time-lag** between the **direct** and **reflected** components in different **energy bands** and at different **Fourier frequencies**.

Modelled self-consistently in **Reltrans** (Ingram et al. 2019, Mastroserio et al. 2021).

- Also modelled by others, e.g. Caballero-Garcia et al. (2019)

Applications, see e.g. **mass estimate** of Cygnus X-1 in O'Neill et al. (2025)

How does geometry influence lag?

Geometry principally changes the **light travel time** and the **illumination profile**.

How does geometry influence lag?

Geometry principally changes the **light travel time** and the **illumination profile**.

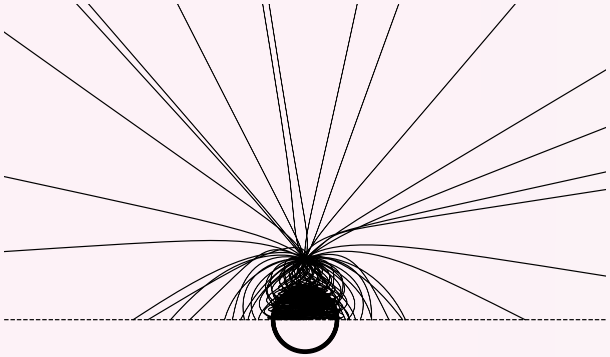

How does geometry influence lag?

Geometry principally changes the **light travel time** and the **illumination profile**.

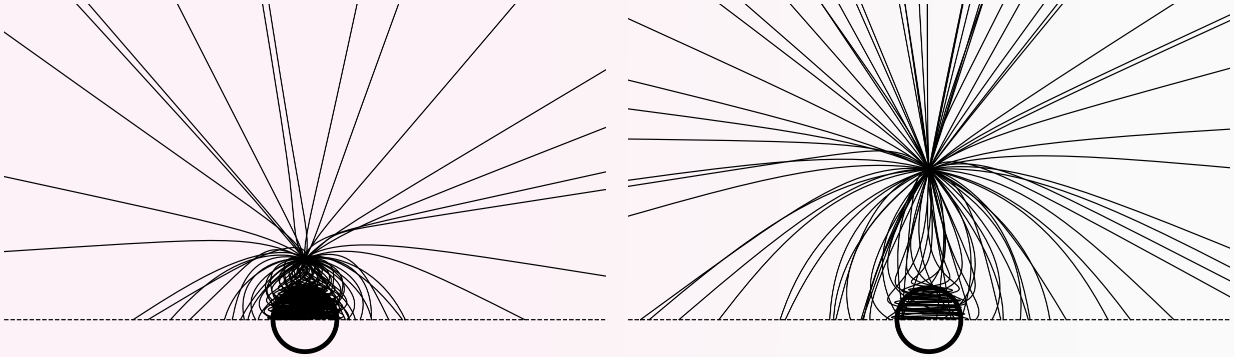

How does geometry influence lag?

Geometry principally changes the **light travel time** and the **illumination profile**.

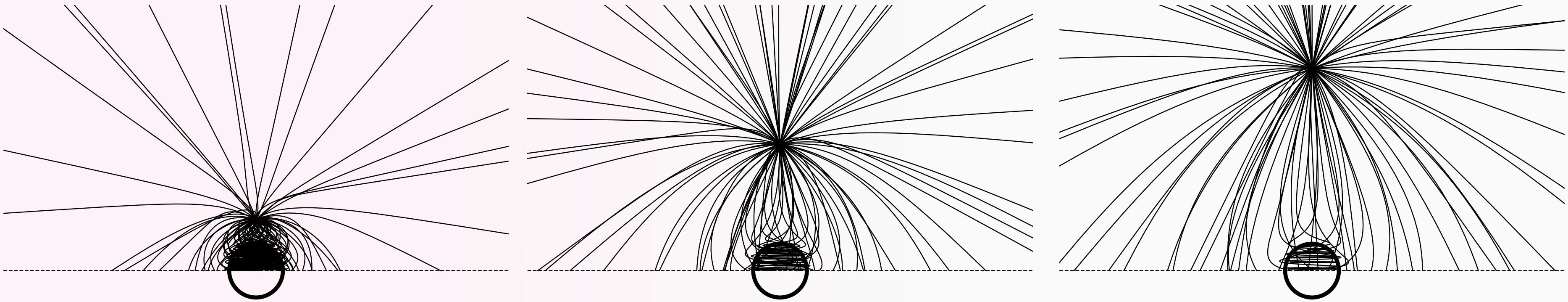

See e.g. Wilkins and Fabian (2012), Gonzalez et al. (2017), Baker (2025)

How does geometry influence lag?

Geometry principally changes the **light travel time** and the **illumination profile**.

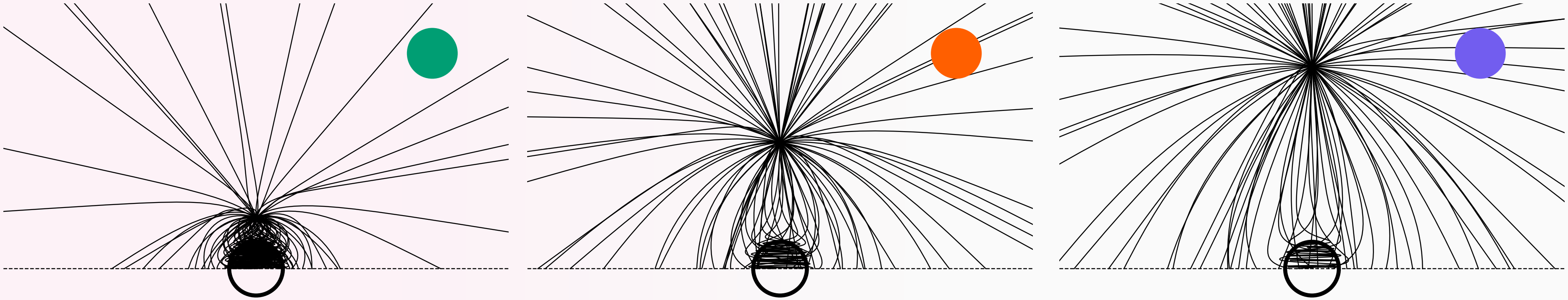

See e.g. Wilkins and Fabian (2012), Gonzalez et al. (2017), Baker (2025)

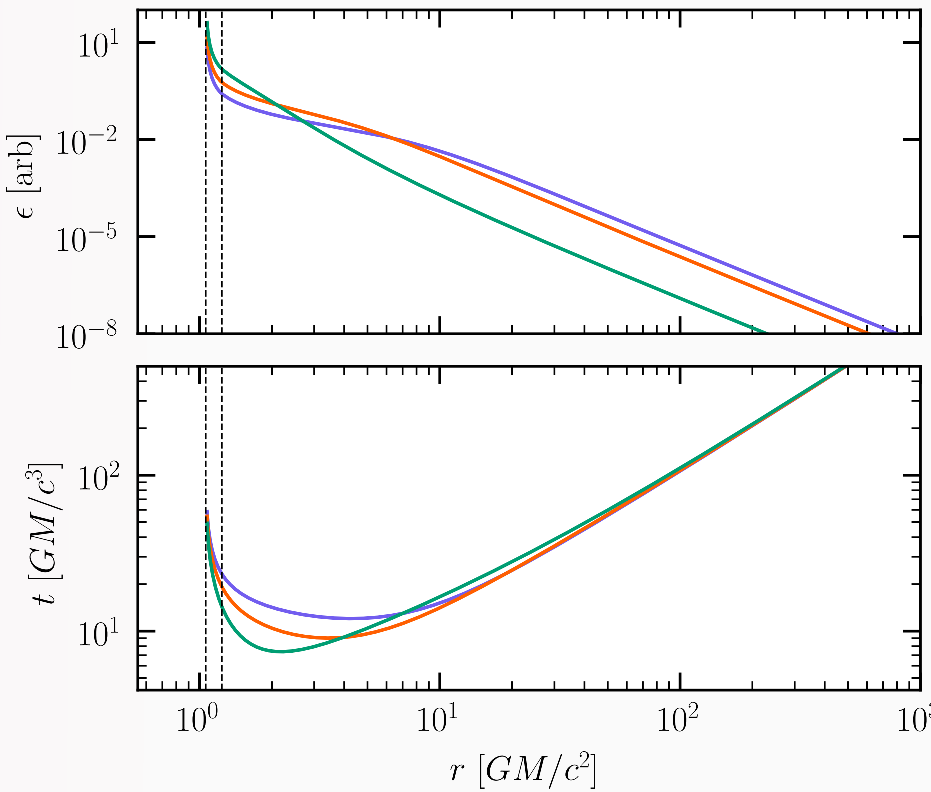

How does geometry influence lag?

Geometry principally changes the **light travel time** and the **illumination profile**.

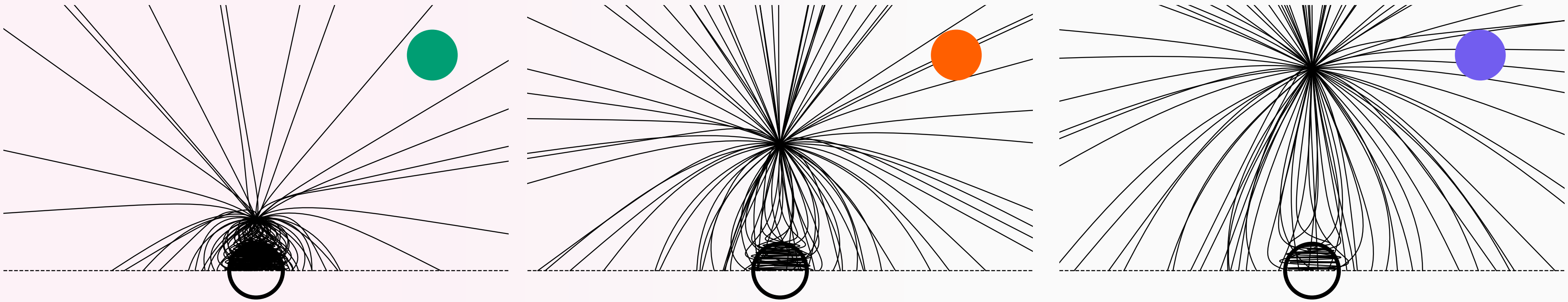

See e.g. Wilkins and Fabian (2012), Gonzalez et al. (2017), Baker (2025)

Extended geometries explored as:

- Double lamppost models Lucchini et al. (2023) and Chainakun and Young (2017)
- Snapshots of extended coronal models Wilkins et al. (2016)

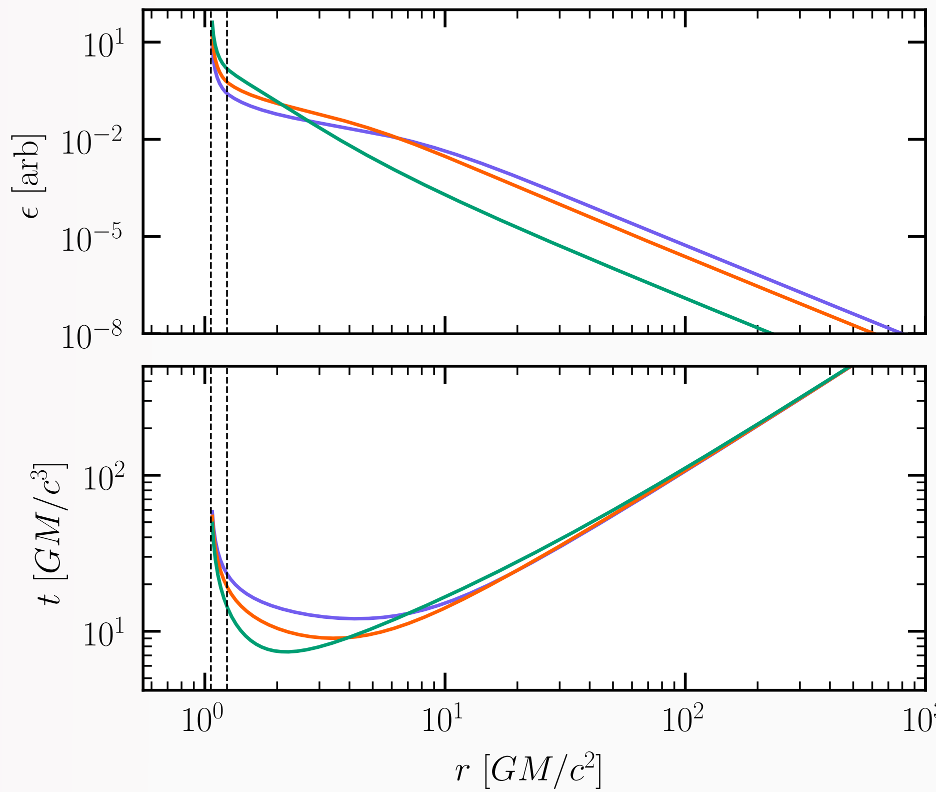

How does geometry influence lag?

Geometry principally changes the **light travel time** and the **illumination profile**.

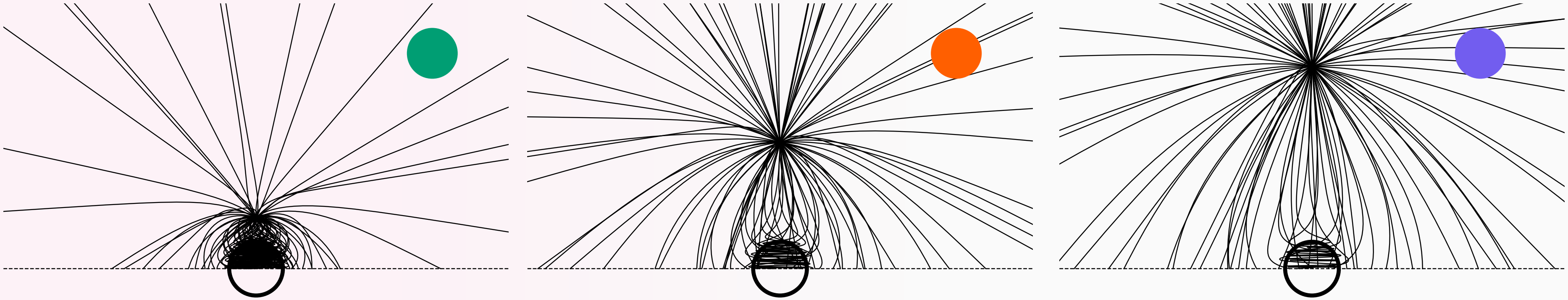

See e.g. Wilkins and Fabian (2012), Gonzalez et al. (2017), Baker (2025)

Extended geometries explored as:

- Double lamppost models Lucchini et al. (2023) and Chainakun and Young (2017)
- Snapshots of extended coronal models Wilkins et al. (2016)

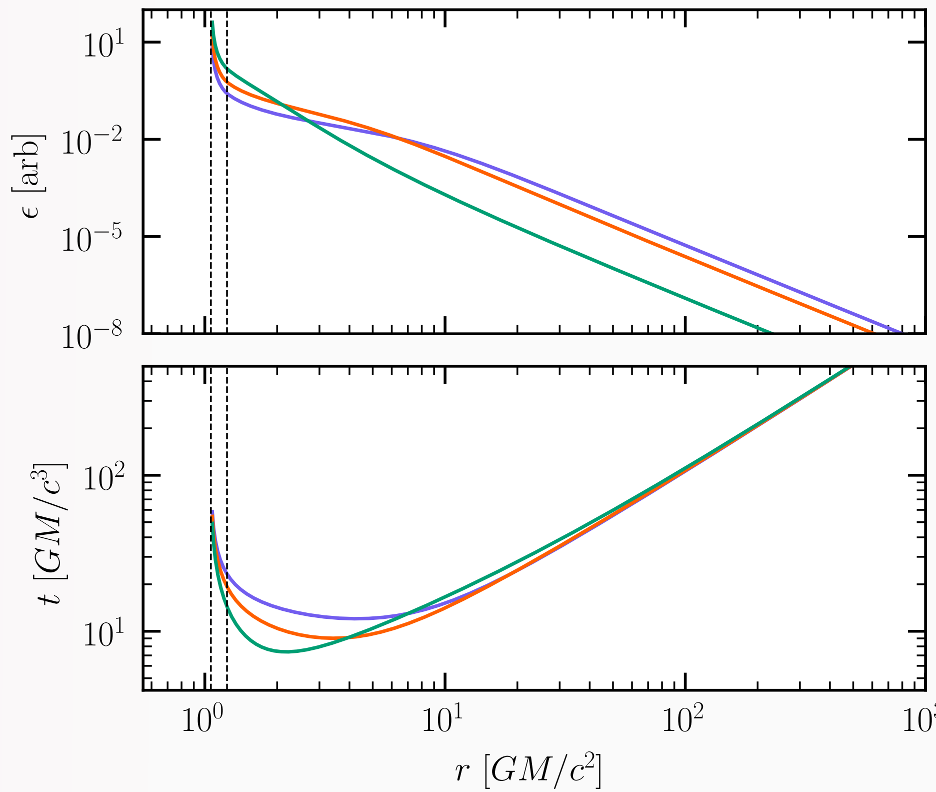

For nearly all models capable of parameter inference, the **lamppost coronal geometry** is used.

Is the lamppost model really so bad?

Is the lamppost model really so bad?

Polarisation results **disfavour** vertically extended / lamppost geometry Krawczynski et al. (2022); Tagliacozzo et al. (2023); Gianolli et al. (2023).

- **Radially extended** geometry is preferred.

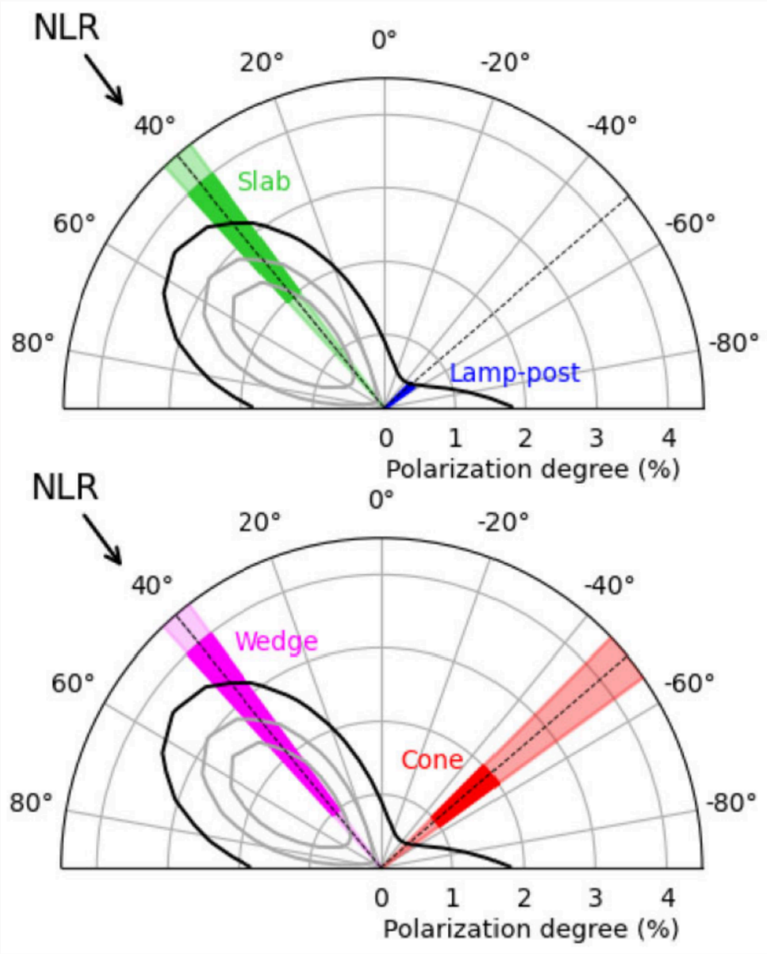

Figure from Tagliacozzo et al. (2023)

Is the lamppost model really so bad?

Polarisation results **disfavour** vertically extended / lamppost geometry Krawczynski et al. (2022); Tagliacozzo et al. (2023); Gianolli et al. (2023).

- **Radially extended** geometry is preferred.

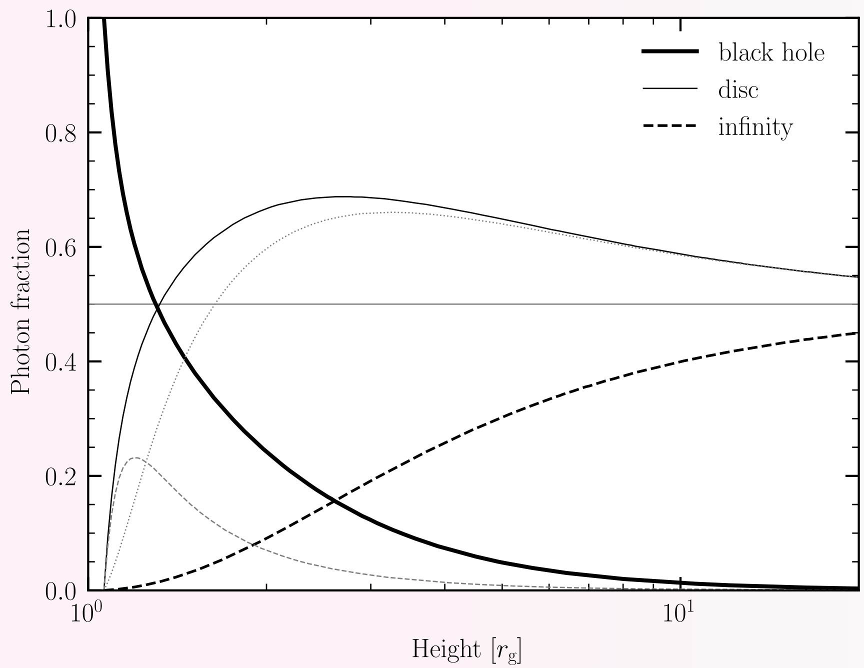

High fraction of **lost photons** when lamppost height is small see also e.g. Dovčiak and Done (2016).

- Ad-hoc "boost" needed to **increase** reflection fraction Dauser et al. (2010); Ingram et al. (2019).

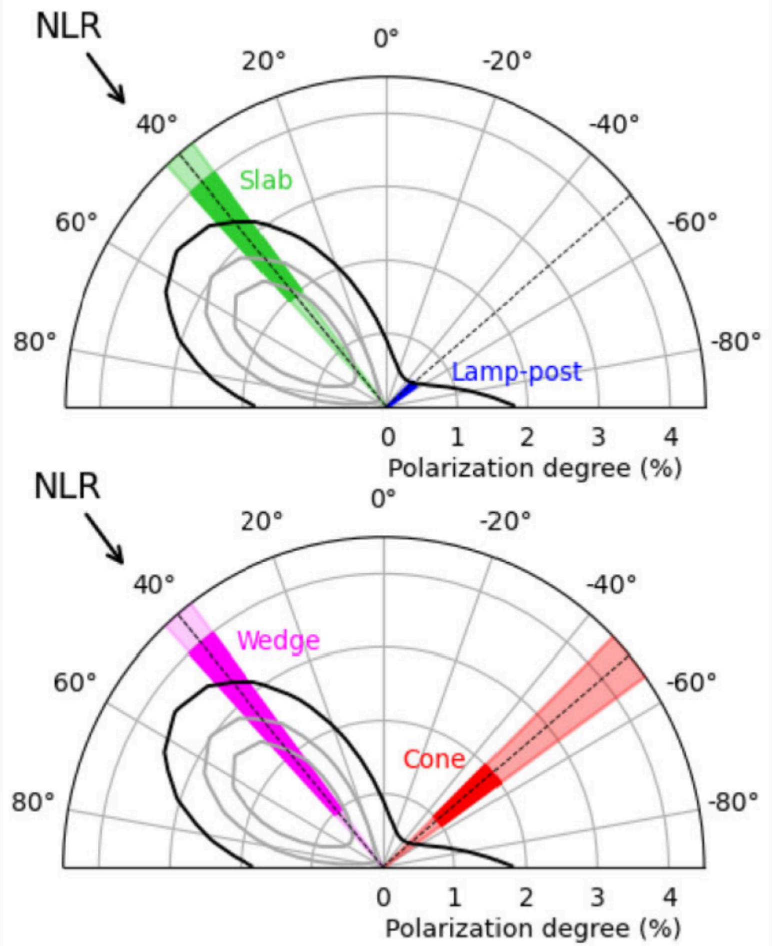

Figure from Tagliacozzo et al. (2023)

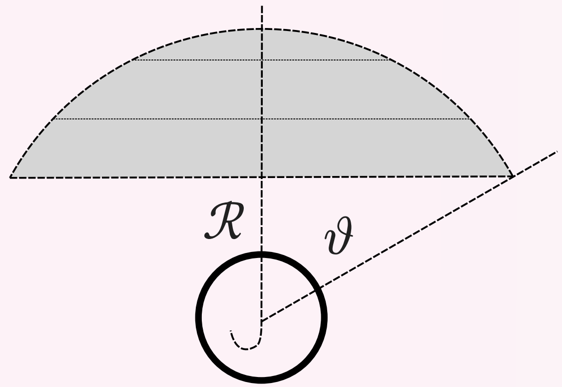

A **lamppost** at height $h = \mathcal{R}$ has an **equivalence class** of extended geometries.

- The "**umbrella**" coronal model e.g. Baker (2025).

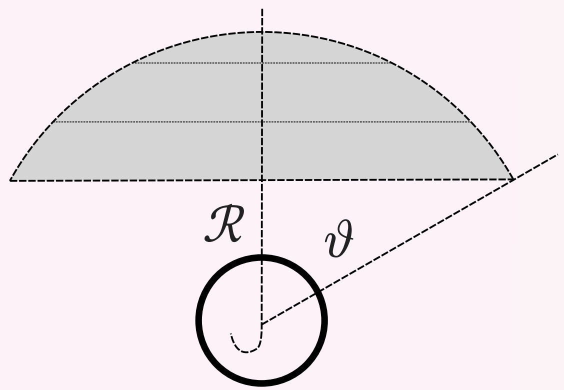

A **lamppost** at height $h = \mathcal{R}$ has an **equivalence class** of extended geometries.

- The "**umbrella**" coronal model e.g. Baker (2025).

Time-averaged umbrella is practically **indistinguishable** from a lamppost (Baker et al., in prep).

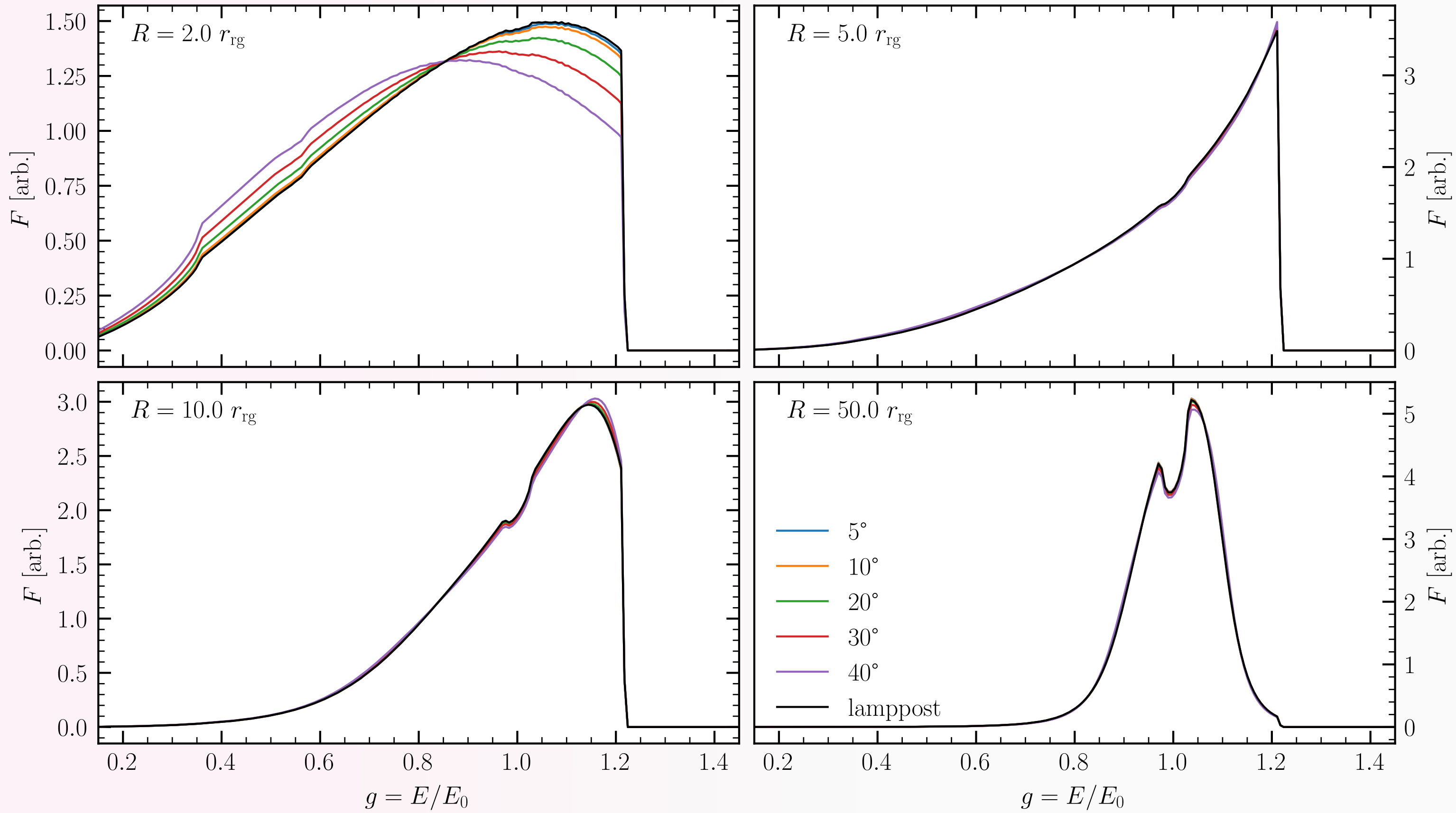

A ring-like corona

Still **axisymmetric**, but the illumining source is now **off-axis**.

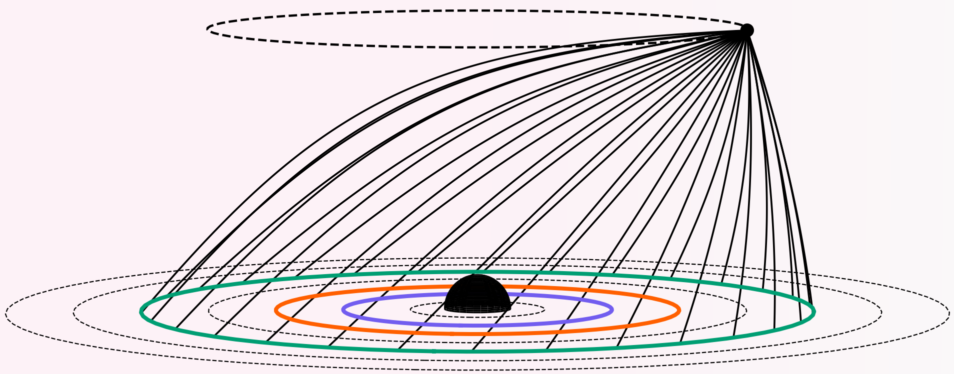

Parameters:

- **Height** h (eqv. Offset R)
- **Radius** x (eqv. Angle ϑ)
- **Velocity factor** v_c

$v_c = 0 \Rightarrow$ stationary
$v_c \leq 1 \Rightarrow$ corotating with disc
$v_c > 1 \Rightarrow$ corotating faster than disc

A ring-like corona

Still **axisymmetric**, but the illumining source is now **off-axis**.

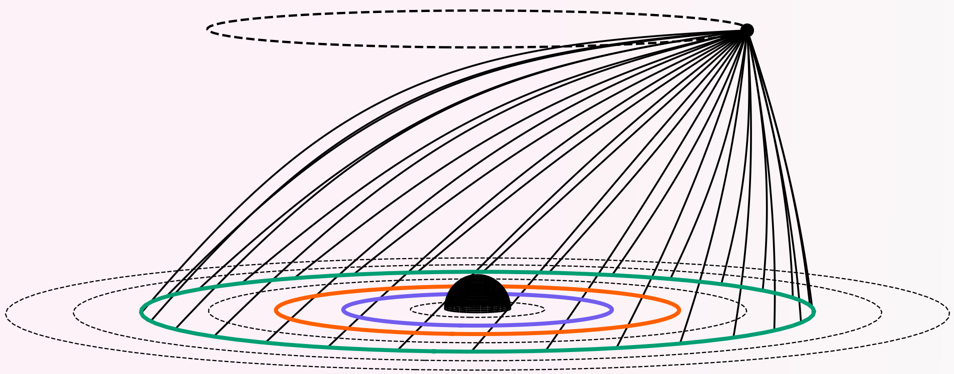

Parameters:

- **Height** h (eqv. Offset R)
- **Radius** x (eqv. Angle ϑ)
- **Velocity factor** v_c

$v_c = 0 \Rightarrow$ stationary
$v_c \leq 1 \Rightarrow$ corotating with disc
$v_c > 1 \Rightarrow$ corotating faster than disc

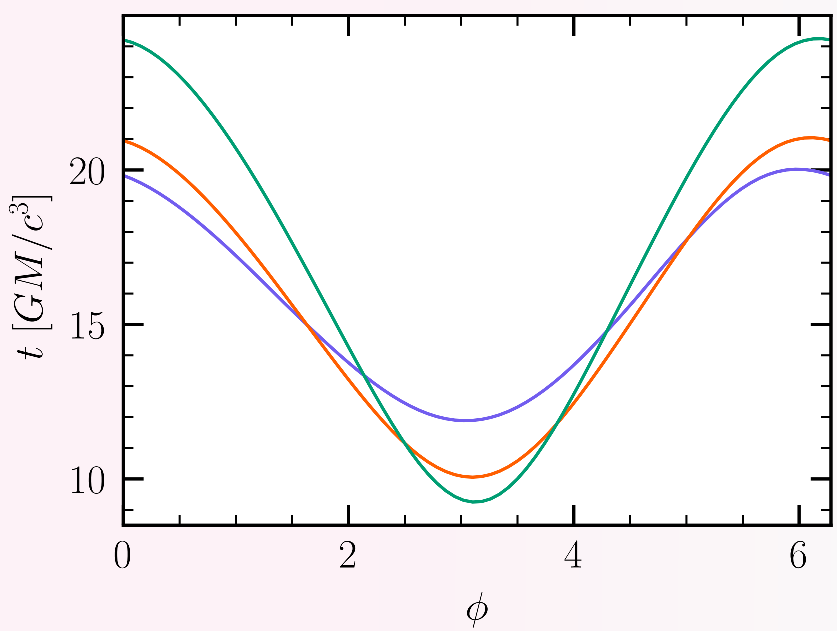

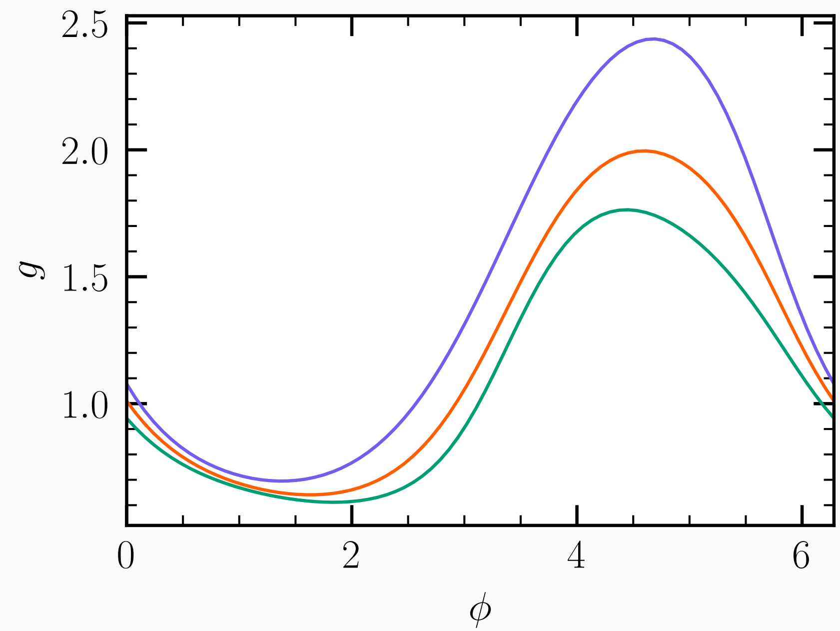

Time-averaged reflection

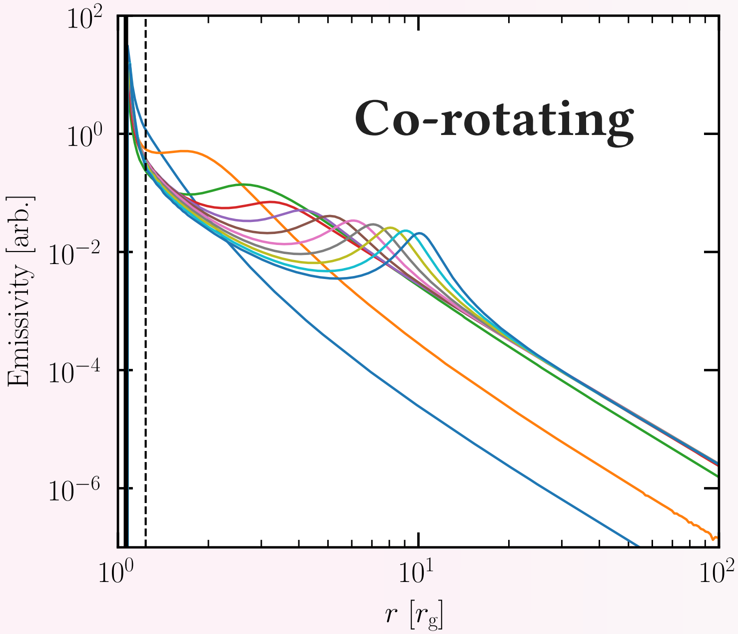

Time-averaged reflection

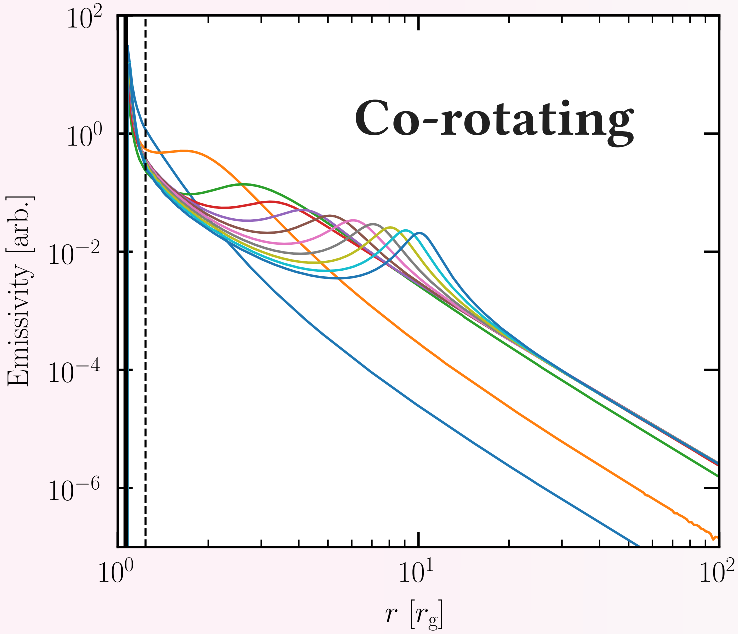

A **ring-like flavour of `relxill`** (`relxill_ring`) developed and fitted in Nekrasov et al. (2025):

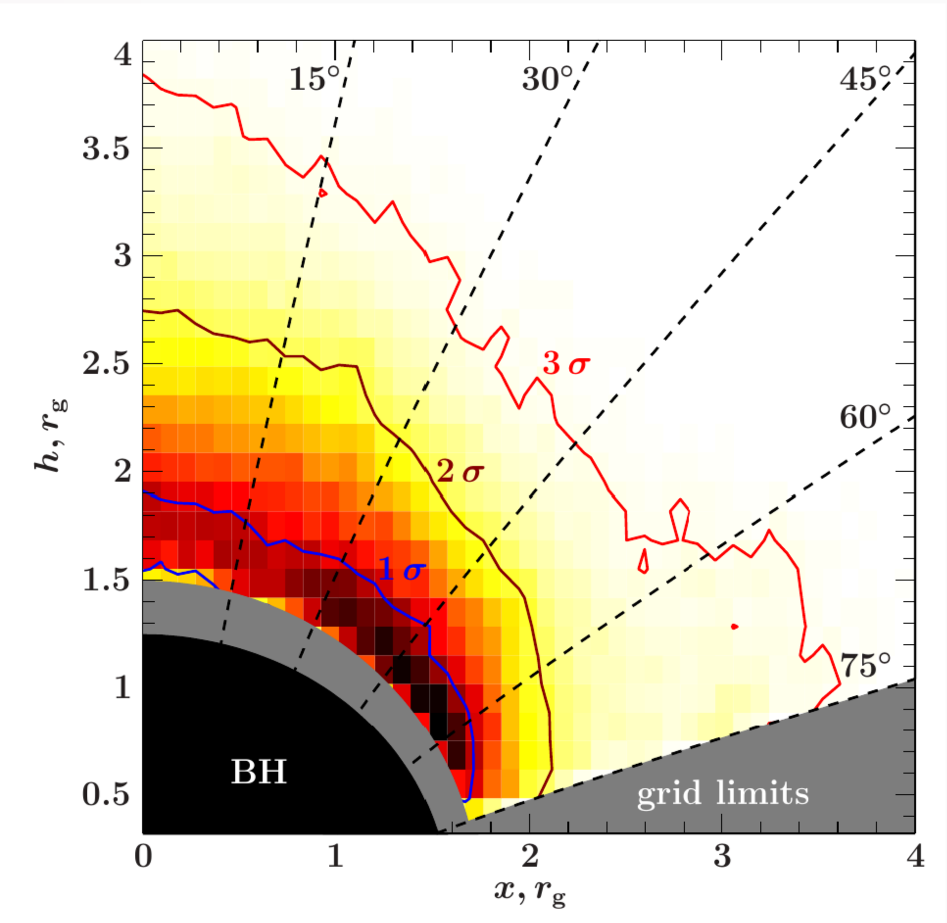

Time-averaged reflection

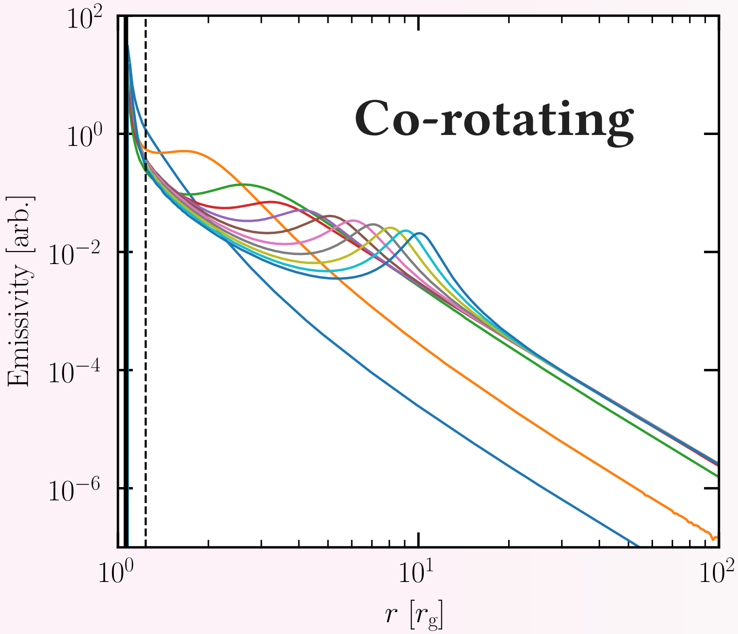

A **ring-like flavour of `relxill`** (`relxill_ring`) developed and fitted in Nekrasov et al. (2025):

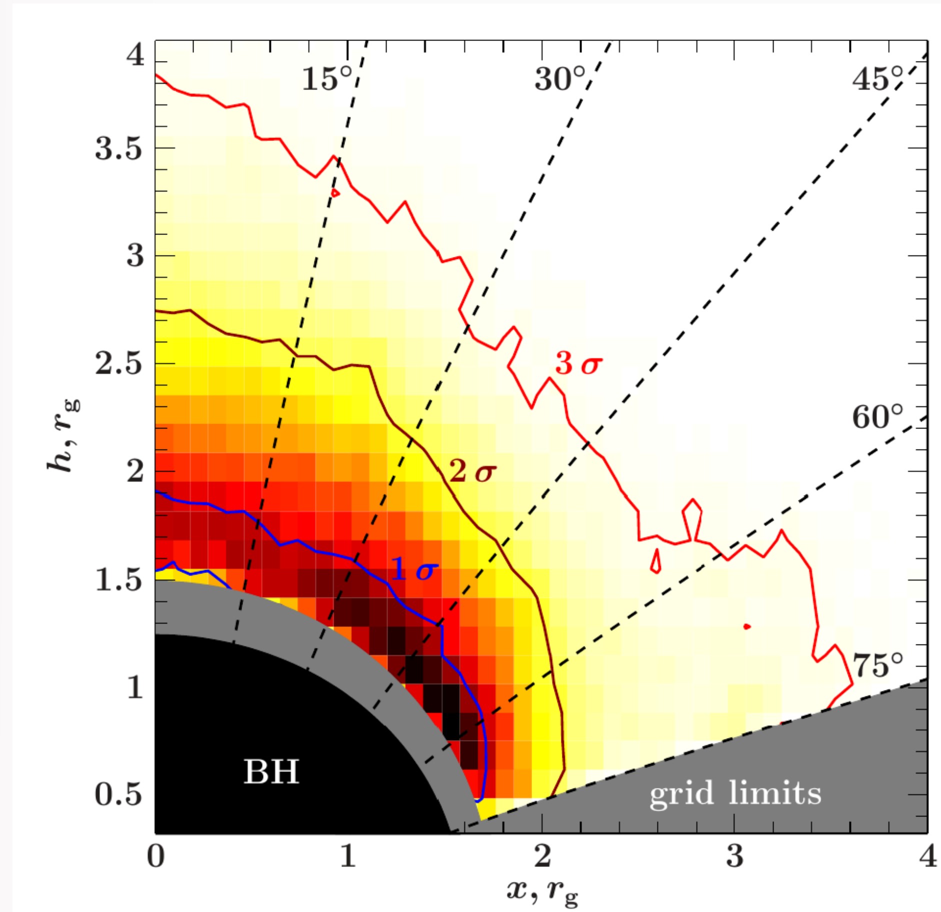

Contours are **umbrella** shells!

Time-averaged reflection

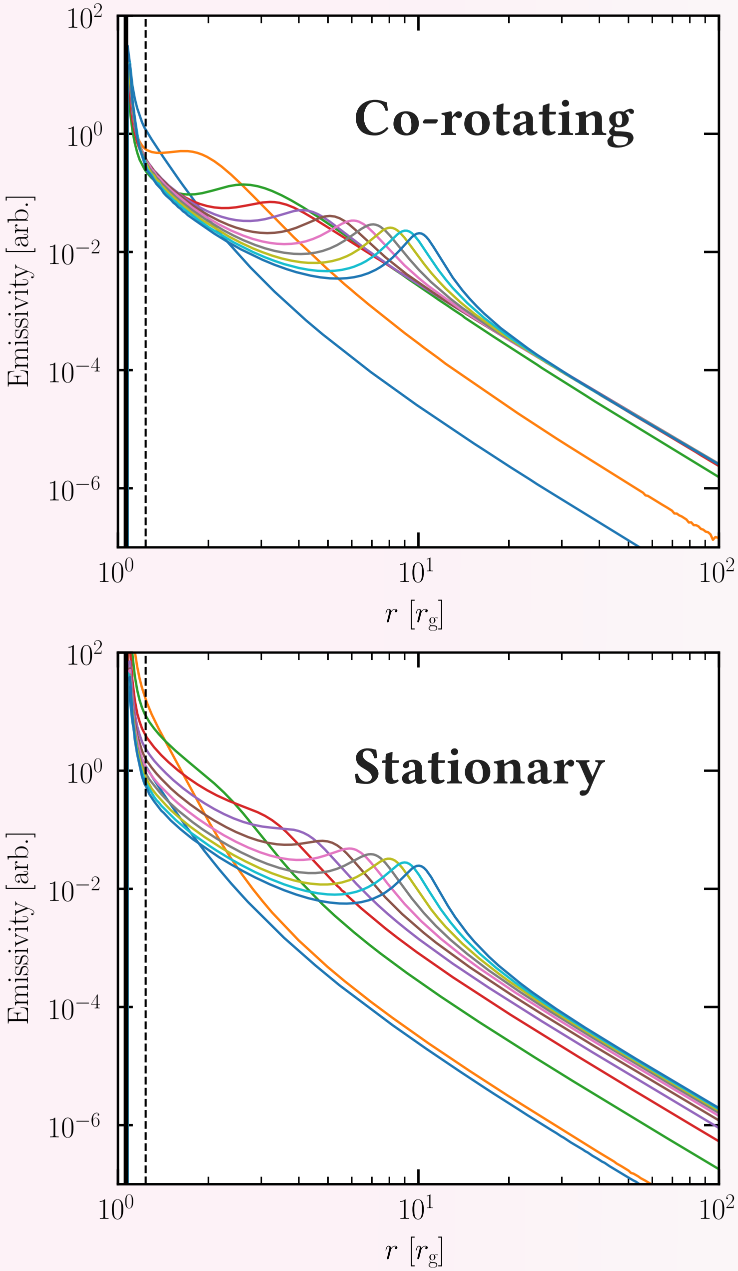

A **ring-like flavour of `relxill`** (`relxill_ring`) developed and fitted in Nekrasov et al. (2025):

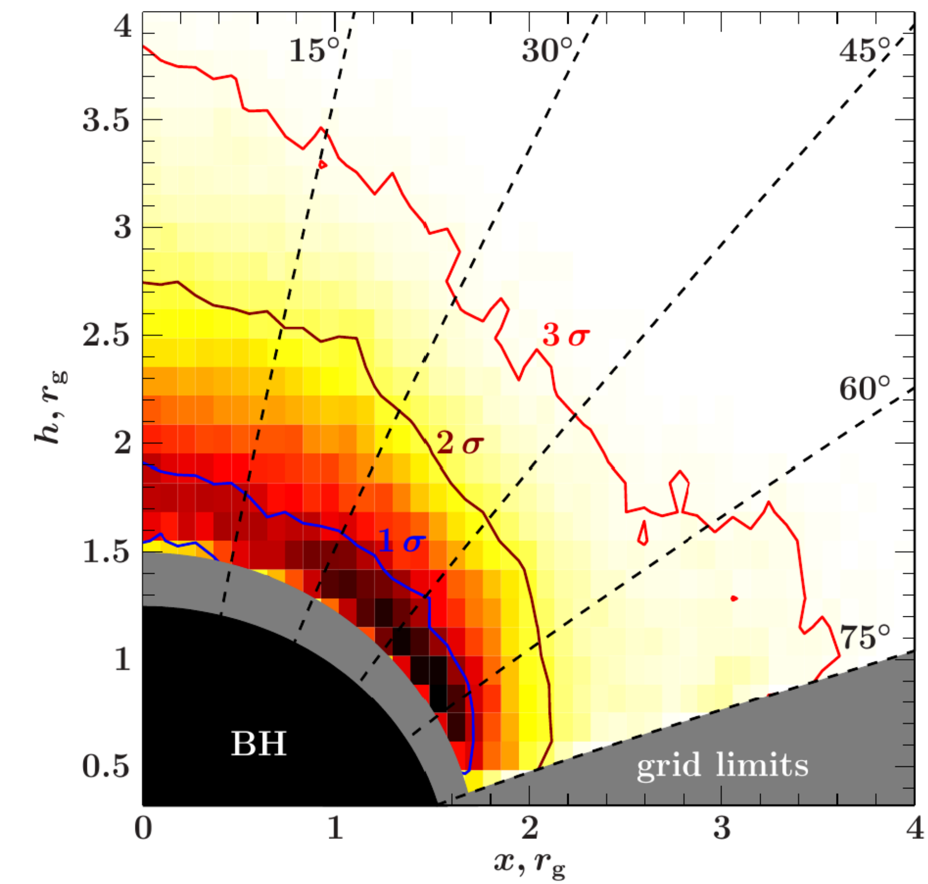

Contours are **umbrella** shells!

Treating the continuum

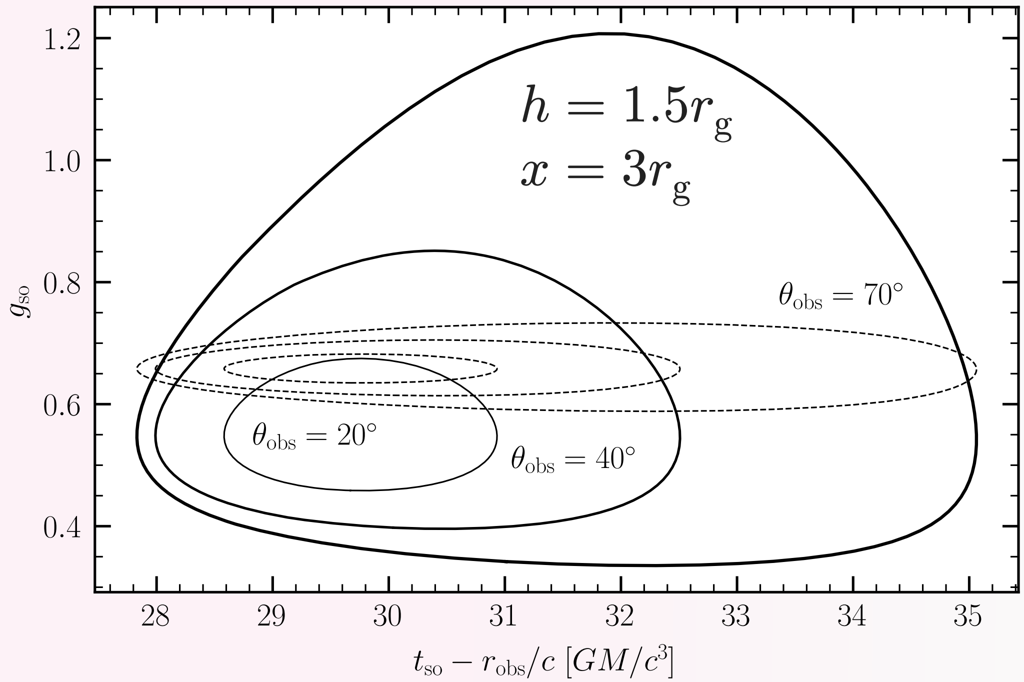

For a **point-like source**:

$$s(t, E) = a(t)c(E) + a(t) \otimes r(\tau, E),$$

where $s(t, E)$ is the **observed light curve**, $a(t)$ is the **common driving process**, $c(E)$ is the **continuum spectrum**, and $r(\tau, E)$ is the **disc impulse response**.

For an **extended source**:

$$s(t, E) = a(t) \otimes c(\tau, E) + a(t) \otimes r(\tau, E),$$

where a convolution with a **continuum** impulse response is also needed.

Treating the continuum

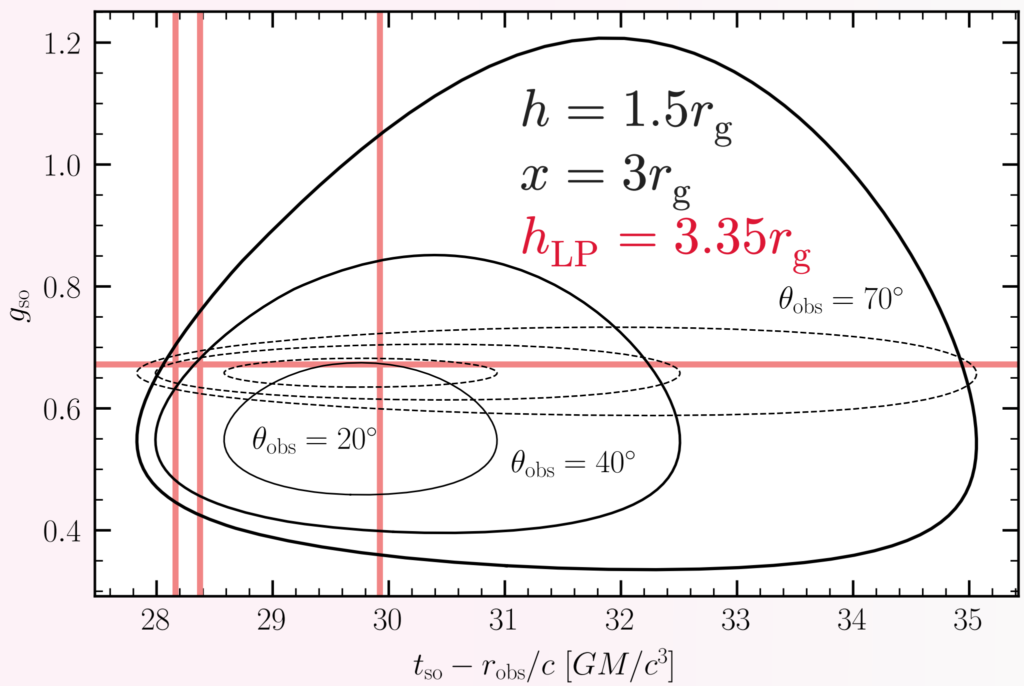

For a **point-like source**:

$$s(t, E) = a(t)c(E) + a(t) \otimes r(\tau, E),$$

where $s(t, E)$ is the **observed light curve**, $a(t)$ is the **common driving process**, $c(E)$ is the **continuum spectrum**, and $r(\tau, E)$ is the **disc impulse response**.

For an **extended source**:

$$s(t, E) = a(t) \otimes c(\tau, E) + a(t) \otimes r(\tau, E),$$

where a convolution with a **continuum** impulse response is also needed.

Treating the continuum

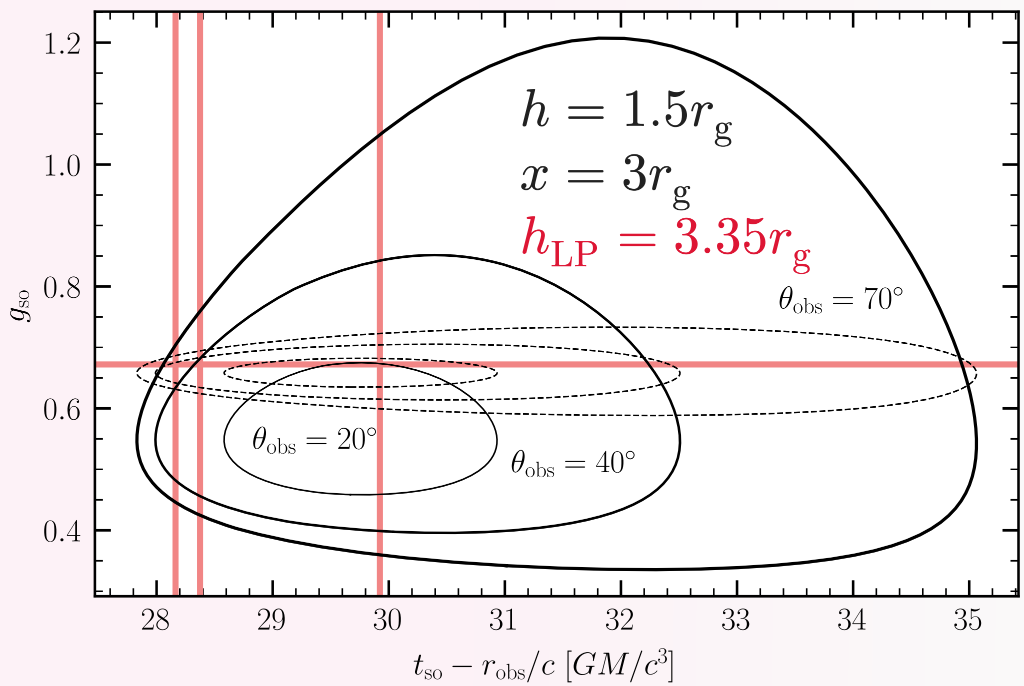

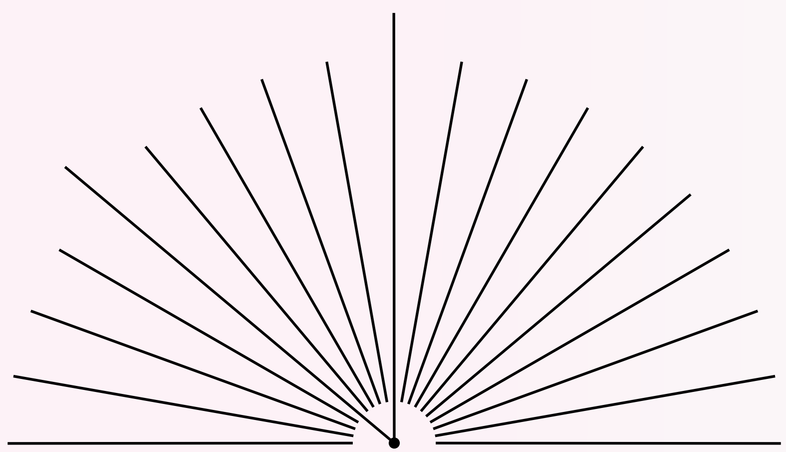

Stationary (all g equal)

For a **point-like source**:

$$s(t, E) = a(t)c(E) + a(t) \otimes r(\tau, E),$$

where $s(t, E)$ is the **observed light curve**, $a(t)$ is the **common driving process**, $c(E)$ is the **continuum spectrum**, and $r(\tau, E)$ is the **disc impulse response**.

For an **extended source**:

$$s(t, E) = a(t) \otimes c(\tau, E) + a(t) \otimes r(\tau, E),$$

where a convolution with a **continuum** impulse response is also needed.

Treating the continuum

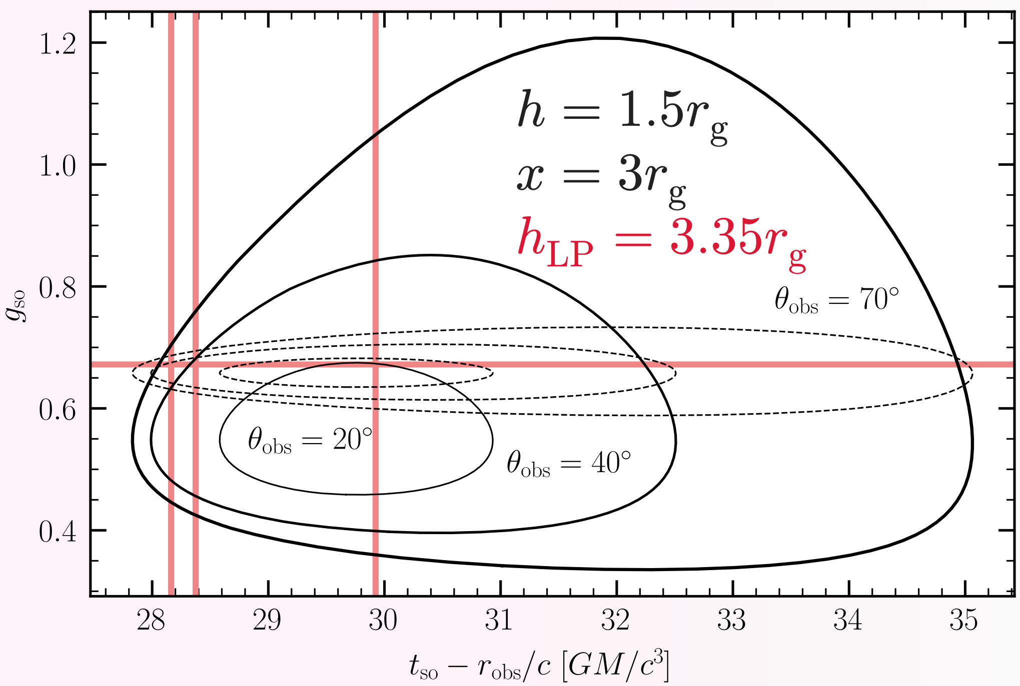

For a **point-like source**:

$$s(t, E) = a(t)c(E) + a(t) \otimes r(\tau, E),$$

where $s(t, E)$ is the **observed light curve**, $a(t)$ is the **common driving process**, $c(E)$ is the **continuum spectrum**, and $r(\tau, E)$ is the **disc impulse response**.

For an **extended source**:

$$s(t, E) = a(t) \otimes c(\tau, E) + a(t) \otimes r(\tau, E),$$

where a convolution with a **continuum** impulse response is also needed.

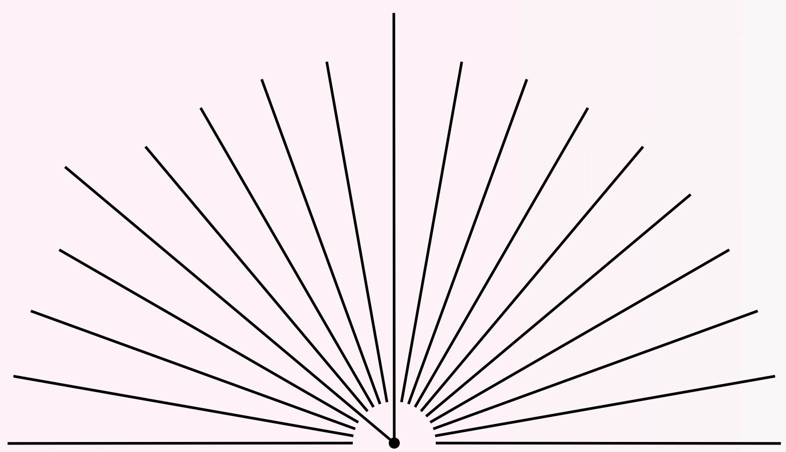

Stationary (all g equal)

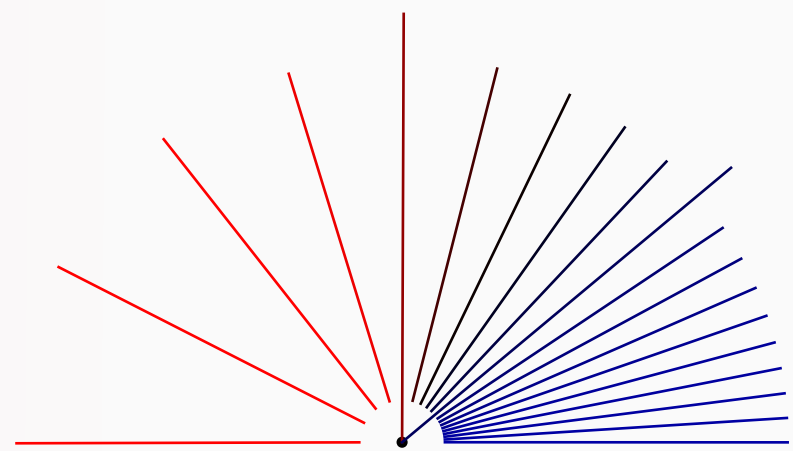

Boosted (g gradient)

Time-resolved reverberation

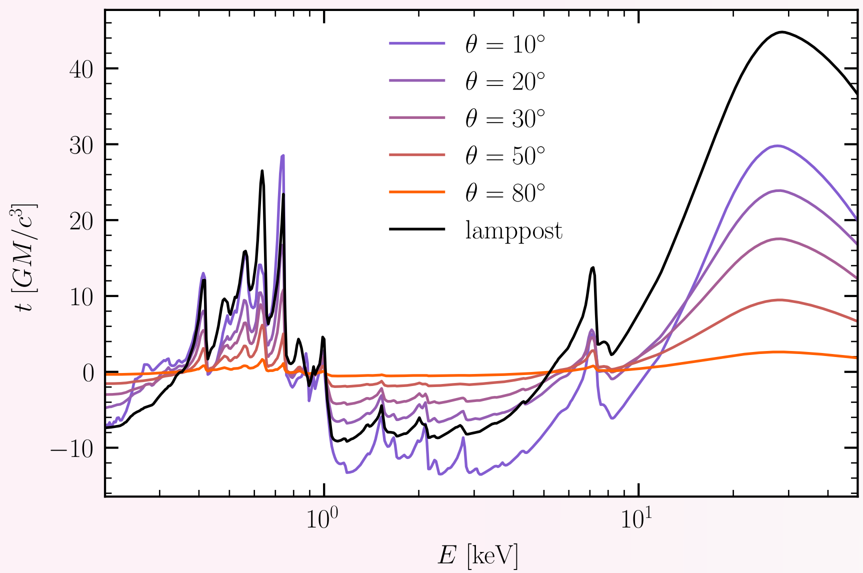

Degeneracy in the time-average is **lifted** by time-resolved spectra.

- The equivalence class in the time-average **is not equivalent** in the reverberation lag.

Time-resolved reverberation

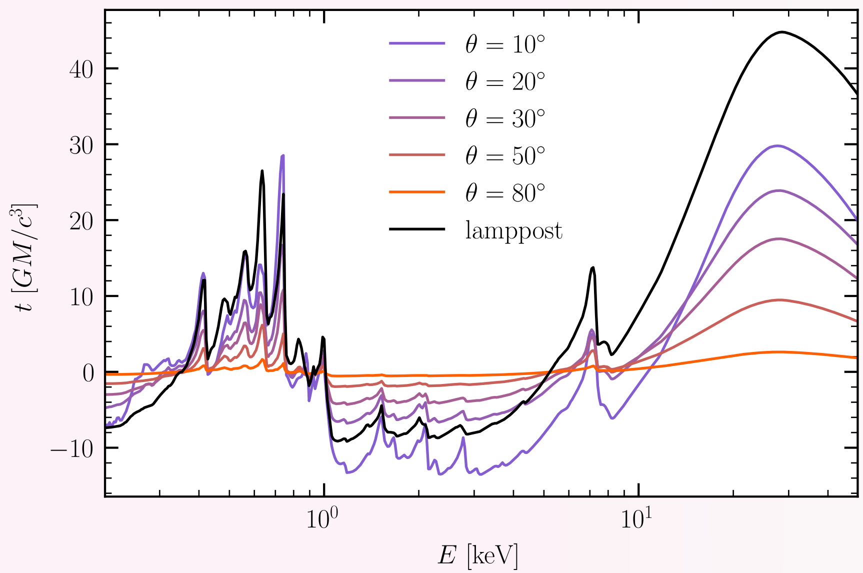

Degeneracy in the time-average is **lifted** by time-resolved spectra.

- The equivalence class in the time-average **is not equivalent** in the reverberation lag.

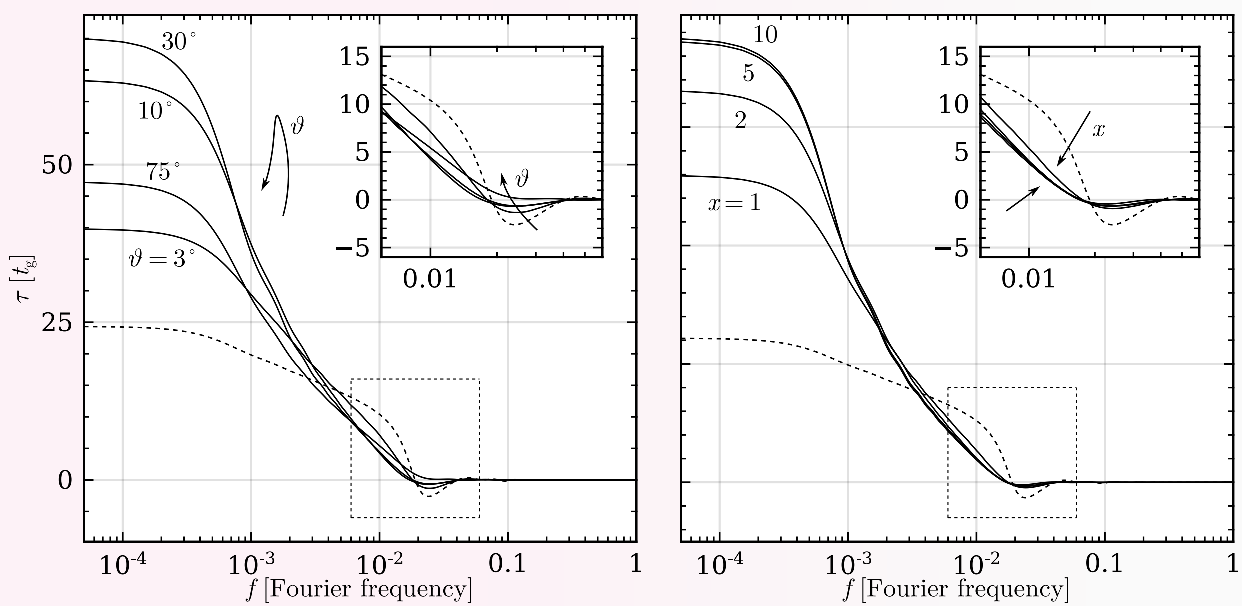

Two expansion modes:

- Fixed R, increase ϑ
  (Low-frequency) lag **increases** then **decreases**.
- Fixed h, increase x
  (Low-frequency) lag **increases**.

Increasing R or h **increases** the lag (analogous to lamppost).

Sensitivity to the velocity profile

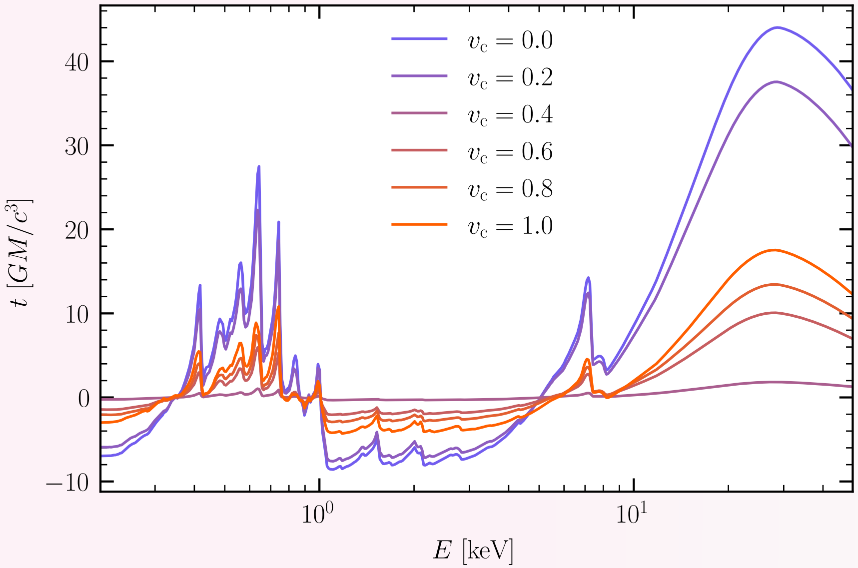

Although velocity **does not** change t, it **changes** g and **flux** $F \propto g^3$.

- Can be made to **dilute** the lag entirely*:

$$\phi(\nu) = \arctan\left(\frac{R \ \mathrm{Im}\ [\Phi(\nu)]}{1 + R \ \mathrm{Re}\ [\Phi(\nu)]}\right),$$

where R is the **reflection fraction**.

* This is our current understanding but we are still investigating.

Sensitivity to the velocity profile

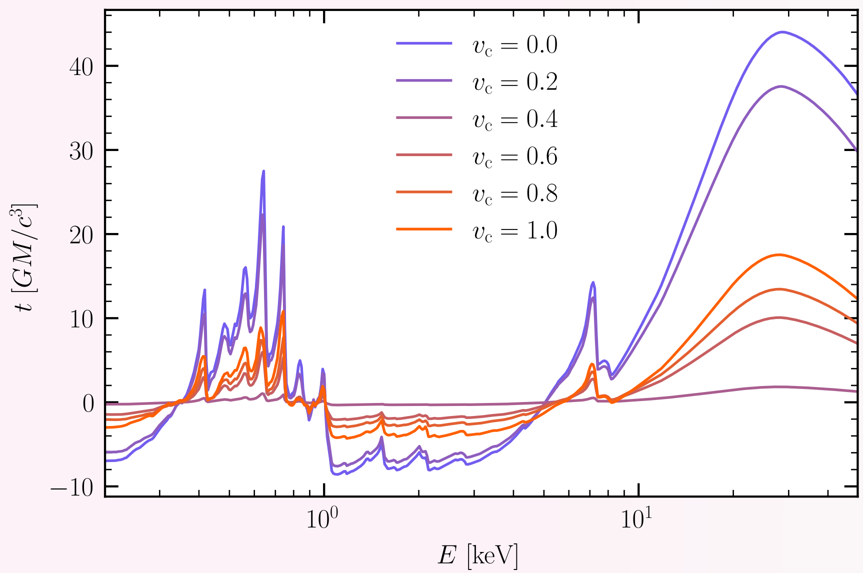

Although velocity **does not** change t, it **changes** g and **flux** $F \propto g^3$.

- Can be made to **dilute** the lag entirely*:

$$\phi(\nu) = \arctan\left(\frac{R \ \mathrm{Im}\left[\Phi(\nu)\right]}{1 + R \ \mathrm{Re}\left[\Phi(\nu)\right]} \right),$$

where R is the **reflection fraction**.

* This is our current understanding but we are still investigating.

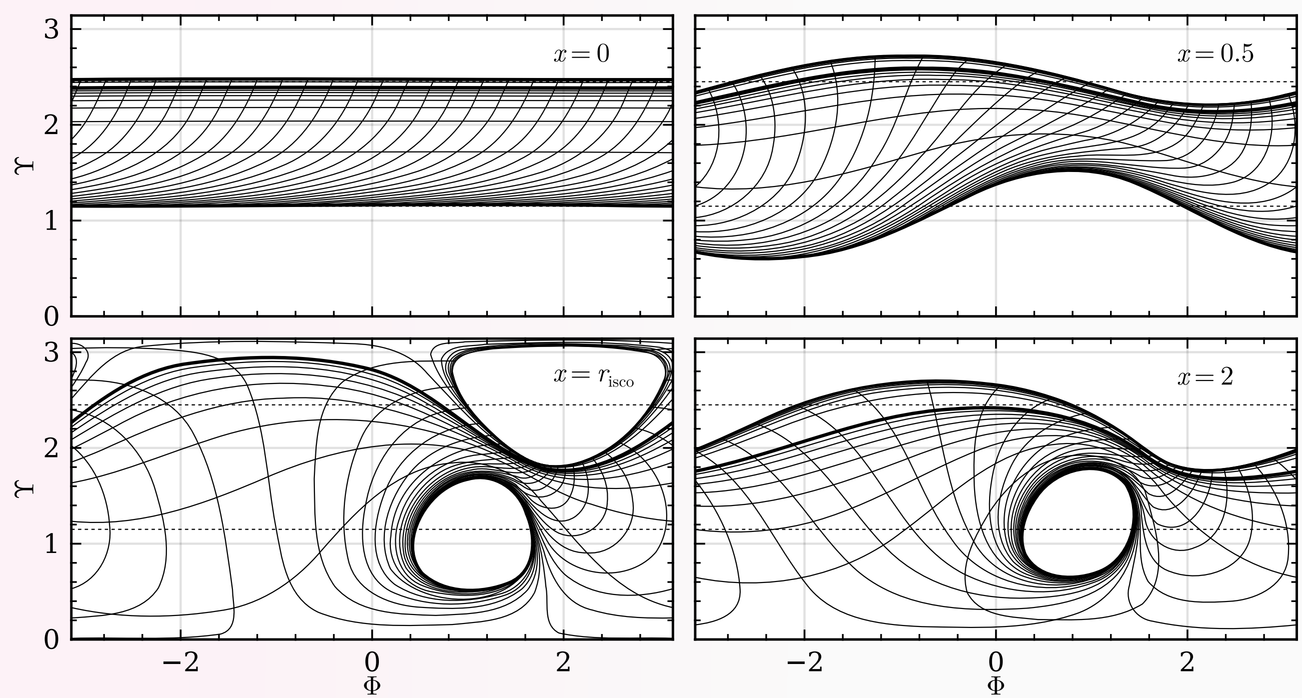

kerrz

A new, open-source (GPL 3.0) general relativistic **ray-tracing library** and **command line tool** for X-ray **spectra**, **timing**, and **polarimetry**:

```
pip install kerrz
# Optional: alias kerrz=kerrzcli
```

Replaced YNOGK … in **Reltrans** with a 10% performance improvement on model evaluation!

- Uses Gralla and Lupsasca (2020) with **automatic differentiation** for fast and efficient gradients.

Source mirror: https://codeberg.org/astro-group/kerrz
Homepage: https://cosroe.com/kerrz

```
# Ring-like emissivity profiles
kerrz emissivity --ring-like h:4,x:3 --velocity corotate --nphotons 500000 -o emissivity.fits

# Reverberation impulse response
kerrz impulse --spin 0.8 --incl 60 --emissivity-profile ./emissivity.fits

# Image of a black hole from a point along the ring
kerrz sky --position h:4,x:3 --velocity corotate --map redshift
```

CLI is FITS in and FITS out.

Written in **Zig**, but distributed with **C / C++**, **Python**, and **Fortran** bindings.

Baker, Nekrasov, Ingram (in prep.)

References

Baker, F. J. E. (2025). *General relativistic effects in black hole X-ray coronal models* [Doctoral dissertation].

Caballero-Garcia, M., Dovciak, M., Bursa, M., Papadakis, I., & Karas, V. (2019). X-ray Reverberation Observational Modelling in Active Galactic Nuclei. *Arxiv E-Prints*, arXiv:1901.04357. https://doi.org/10.48550/arXiv.1901.04357

Chainakun, P., & Young, A. (2017). Investigating the X-ray time lags in PG 1244+026 using an extended corona model. \mnras, *465*(4), 3965–3976. https://doi.org/10.1093/mnras/stw2964

Chainakun, P., Young, A., & Kara, E. (2016). Relativistic X-ray reverberation modelling of the combined time-averaged and lag-energy spectra in AGN. \mnras, *460*(3), 3076–3088. https://doi.org/10.1093/mnras/stw1105

Dauser, T., Wilms, J., Reynolds, C., & Brenneman, L. (2010). Broad emission lines for a negatively spinning black hole. \mnras, *409*(4), 1534–1540. https://doi.org/10.1111/j.1365-2966.2010.17393.x

Dovčiak, M., & Done, C. (2016). Minimum X-ray source size of the on-axis corona in AGN. *Astronomische Nachrichten*, *337*(4–5), 441. https://doi.org/10.1002/asna.201612327

Fabian, A., Rees, M., Stella, L., & White, N. (1989). X-ray fluorescence from the inner disc in Cygnus X-1. \mnras, *238*, 729–736. https://doi.org/10.1093/mnras/238.3.729

Gianolli, V., Kim, D., Bianchi, S., Ag\'is-González, B., Madejski, G., Marin, F., Marinucci, A., Matt, G., Middei, R., Petrucci, P.-O., Soffitta, P., Tagliacozzo, D., Tombesi, F., Ursini, F., Barnouin, T., De Rosa, A., Di Gesu, L., Ingram, A., Loktev, V., … Zane, S. (2023). Uncovering the geometry of the hot X-ray corona in the Seyfert galaxy NGC 4151 with IXPE. \mnras, *523*(3), 4468–4476. https://doi.org/10.1093/mnras/stad1697

Gonzalez, A., Wilkins, D., & Gallo, L. (2017). Probing the geometry and motion of AGN coronae through accretion disc emissivity profiles. \mnras, *472*(2), 1932–1945. https://doi.org/10.1093/mnras/stx2080

Gralla, S. E., & Lupsasca, A. (2020). Null geodesics of the Kerr exterior. \prd, *101*(4), 44032. https://doi.org/10.1103/PhysRevD.101.044032

Ingram, A., Mastroserio, G., Dauser, T., Hovenkamp, P., van der Klis, M., & García, J. A. (2019). A public relativistic transfer function model for X-ray reverberation mapping of accreting black holes. \mnras, *488*(1), 324–347. https://doi.org/10.1093/mnras/stz1720

Krawczynski, H., Muleri, F., Dovčiak, M., Veledina, A., Rodriguez Cavero, N., Svoboda, J., Ingram, A., Matt, G., Garcia, J. A., Loktev, V., Negro, M., Poutanen, J., Kitaguchi, T., Podgorný, J., Rankin, J., Zhang, W., Berdyugin, A., Berdyugina, S. V., Bianchi, S., … Zane, S. (2022). Polarized x-rays constrain the disk-jet geometry in the black hole x-ray binary Cygnus X-1. *Science*, *378*(6620), 650–654. https://doi.org/10.1126/science.add5399

Lucchini, M., Mastroserio, G., Wang, J., Kara, E., Ingram, A., Garcia, J., Dauser, T., van der Klis, M., König, O., Lewin, C., Nathan, E., & Panagiotou, C. (2023). Investigating the Impact of Vertically Extended Coronae on X-Ray Reverberation Mapping. \apj, *951*(1), 19. https://doi.org/10.3847/1538-4357/acd24f

Mastroserio, G., Ingram, A., Wang, J., Garc\ia, J. A., van der Klis, M., Cavecchi, Y., Connors, R., Dauser, T., Harrison, F., Kara, E., König, O., & Lucchini, M. (2021). Modelling correlated variability in accreting black holes: the effect of high density and variable ionization on reverberation lags. \mnras, *507*(1), 55–73. https://doi.org/10.1093/mnras/stab2056

Nekrasov, A., Dauser, T., Garc\ia, J., Walton, D., Fromm, C., Young, A., Baker, F., Joyce, A., König, O., Licklederer, S., Häfner, J., & Wilms, J. (2025). Relativistic reflection within an extended hot plasma geometry. \aap, *704*, A129. https://doi.org/10.1051/0004-6361/202556012

O'Neill, P., Ingram, A., Nathan, E., Mastroserio, G., van der Klis, M., Lucchini, M., & Mitchell, J. (2025). X-ray reverberation black hole mass and distance estimates of Cygnus X-1. *Arxiv E-Prints*, arXiv:2501.12788. https://doi.org/10.48550/arXiv.2501.12788

Reynolds, C. S., Young, A. J., Begelman, M. C., & Fabian, A. C. (1999). X-Ray Iron Line Reverberation from Black Hole Accretion Disks. \apj, *514*(1), 164–179. https://doi.org/10.1086/306913

Tagliacozzo, D., Marinucci, A., Ursini, F., Matt, G., Bianchi, S., Baldini, L., Barnouin, T., Cavero Rodriguez, N., De Rosa, A., Di Gesu, L., Dovčiak, M., Harper, D., Ingram, A., Karas, V., Kim, D., Krawczynski, H., Madejski, G., Marin, F., Middei, R., … Zane, S. (2023). The geometry of the hot corona in MCG-05-23-16 constrained by X-ray polarimetry. \mnras, *525*(3), 4735–4743. https://doi.org/10.1093/mnras/stad2627

Uttley, P., Cackett, E., Fabian, A., Kara, E., & Wilkins, D. (2014). X-ray reverberation around accreting black holes. \aapr, *22*, 72. https://doi.org/10.1007/s00159-014-0072-0

Wilkins, D., & Fabian, A. (2012). Understanding X-ray reflection emissivity profiles in AGN: locating the X-ray source. \mnras, *424*(2), 1284–1296. https://doi.org/10.1111/j.1365-2966.2012.21308.x

Wilkins, D., Cackett, E., Fabian, A., & Reynolds, C. (2016). Towards modelling X-ray reverberation in AGN: piecing together the extended corona. \mnras, *458*(1), 200–225. https://doi.org/10.1093/mnras/stw276

Zoghbi, A., Fabian, A., Reynolds, C., & Cackett, E. (2012). Relativistic iron K X-ray reverberation in NGC 4151. \mnras, *422*(1), 129–134. https://doi.org/10.1111/j.1365-2966.2012.20587.x

Summary

Ring **angle**

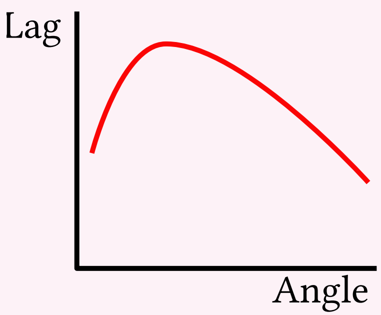

Ring **radius**

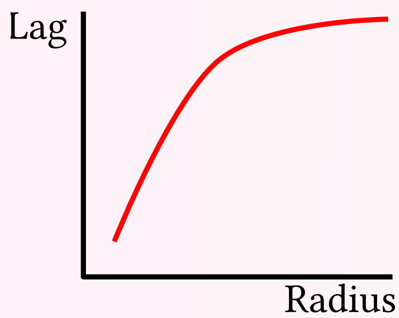

Ring **velocity**

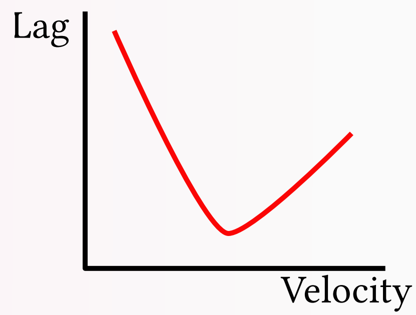

GitHub Reltrans Org:
github.com/reltrans/reltrans

Codeberg kerrz:
codeberg.org/astro-group/kerrz

Reltrans has a **new ring-like coronal model** that you can fit to data (soon!).

- Three parameters for the coronal geometry: **height**, **radius**, and **velocity profile**.
- Assumed velocity profile can **dramatically change** spectra and lags.

> Combined spectral-timing **will be able to constrain** coronal geometry.

Contact:
fergus.j.baker@durham.ac.uk
https://cosroe.com

Slides and material:
https://codeberg.org/fjebaker/cefalu-2026

Figures rendered using Matplotlib and GNUPlot.
Fonts: Adelphe Germinal (OFL), Libertinus Serif (OFL).
Slides made with Typst.